GeoHealth

RESEARCH ARTICLE
10.1029/2022GH000725

Key Points:

- The Universal Thermal Climate Index and heat stress frequency greatly increased both at summer daytime and nighttime in Beijing-Tianjin-Hebei (BTH)
- A Composite Thermal Comfort Score was proposed to evaluate the long-term, summertime, regional outdoor thermal comfort (OTC)
- The general summertime OTC in BTH showed a decreasing north-south gradient pattern, and a tendency toward the worse

Supporting Information:

Supporting Information may be found in the online version of this article.

Correspondence to:

S. Shen and M. Zhao,
shens@bnu.edu.cn;
zhaomin@bnu.edu.cn

Citation:

Huang, J., Shen, S., Zhao, M., & Cheng, C. (2023). Assessment of summer regional outdoor heat stress and regional comfort in the Beijing-Tianjin-Hebei agglomeration over the last 40 years. *GeoHealth*, *7*, e2022GH000725. https://doi.org/10.1029/2022GH000725

Received 6 JUL 2022
Accepted 1 DEC 2022

Assessment of Summer Regional Outdoor Heat Stress and Regional Comfort in the Beijing-Tianjin-Hebei Agglomeration Over the Last 40 Years

Junwang Huang[1,2,3], Shi Shen[1,2,3], Min Zhao[2,3], and Changxiu Cheng[1,2,4]

[1]Key Laboratory of Environmental Change and Natural Disaster, Beijing Normal University, Beijing, China, [2]State Key Laboratory of Earth Surface Processes and Resource Ecology, Beijing Normal University, Beijing, China, [3]Center for Geodata and Analysis, Faculty of Geographical Science, Beijing Normal University, Beijing, China, [4]National Tibetan Plateau Data Center, Beijing, China

Abstract Outdoor thermal comfort (OTC) is critical for public health, labor productivity, and human life. Growing extreme heat events caused by climate change have a serious impact on OTCs, especially in urban areas. Quantitatively characterizing and evaluating the spatiotemporal changes in OTCs are essential, and more applications are needed in urban agglomerations. Therefore, taking the Beijing-Tianjin-Hebei (BTH) urban agglomeration as the study area, this study aimed to quantitatively assess the summer regional OTC from 1981 to 2020. First, the Universal Thermal Climate Index (UTCI) was used as the indicator of daily thermal stress, and then a Composite Thermal Comfort Score was proposed to evaluate the long-term, summertime, regional OTC considering the extent, duration, and intensity of daytime and nighttime thermal stress. The results showed that (a) the increase in UTCI (0.32°C/10a at daytime and 0.21°C/10a at nighttime) and heat stress frequency (0.88 at daytime and 0.39 d/10a at nighttime) were manifested over BTH, indicating a worse OTC. Spatial and temporal heterogeneity was also demonstrated. (b) The general OTC showed a decreasing north-south gradient pattern. At daytime, the northern mountainous zone presented the best OTC, the southern plain zone, especially Hengshui, Langfang, and Cangzhou, showed the worst. At nighttime, the mountain-plain transition zone showed the best OTC, the northern mountainous zone showed the worst since more cold stress occurred. Our findings will be useful in informing climate change adaptation strategies to ensure urban resilience as extreme heat increases in the context of climate change.

Plain Language Summary Outdoor thermal comfort (OTC) in urban areas is getting worse since more extreme heat events occurred. Here, we developed a Composite Thermal Comfort Score, which considering the extent, duration, and intensity of thermal stress assessed by the Universal Thermal Climate Index (UTCI), to evaluate long-term, summertime, regional OTC in the Beijing-Tianjin-Hebei (BTH) urban agglomeration in summer from 1981 to 2020. We found that BTH showed increasing UTCI and growing heat stress frequency both at daytime and nighttime, with spatial and temporal heterogeneity, indicating the worse OTC performance. The general OTC in BTH showed a decreasing north-south gradient pattern. At daytime, the northern mountainous zone showed the best OTC, and the southern plain zone shows the worst. At night, the mountain-plain transition zone shows the best OTC, and the northern mountainous zone shows the worst. This work illustrates a general spatiotemporal pattern of the OTC at the urban agglomeration scale.

1. Introduction

Outdoor thermal comfort (OTC), indicating the bioclimatic condition where the human organism can maintain its thermal balance best in such situations without facing an energy shortage or energy surplus (Adrian et al., 2008). It is an essential parameter to assess the quality of the regional bioclimate and provide guidelines for sustainability. OTC could be evaluated by the thermal stress levels, and the heat stress levels are more decisive for summertime OTC. While extreme heat stress (EHS) is getting more frequent and intensive under climate change (Dosio et al., 2018; Ma et al., 2020; Park & Jeong, 2022; Perkins-Kirkpatrick & Lewis, 2020; Shen et al., 2018). Some regions will suffer more frequent, intensive, and longer extreme heat during summer (Bian et al., 2022; Dosio, 2017; Q. Li et al., 2022; Tomczyk & Owczarek, 2020; Y. Zhang et al., 2022). Changes were particularly evident in the last decade, which has been declared the warmest decade since the preindustrial era, and globally, the air temperature increased by approximately 1.09°C on average in 2011–2020 compared to 1850–1900 and

is projected to continue to increase during the 21st century (Arias et al., 2021). Kang and Eltahir reported that the North China Plain is likely to be unsuitable for working outdoors due to more deadly heatwaves (Kang & Eltahir, 2018). It is accompanied by a severe impact on summertime OTC (Coccolo et al., 2016).

The summertime OTC is deteriorating in many parts of the world according to projection, and pose great threats on outdoor working efficiency (Burke et al., 2015), tourism (Sahabi Abed & Matzarakis, 2018), and human health (Kuchcik, 2017). Koteswara Rao et al. (2020) projected a 30%–40% decline in the work performed in India by the end of the century due to elevated heat stress levels. A study of the Zayandehroud River route from 2014 to 2039 showed that some tourism destinations in the western part of the river are at risk of a reduction in the number of climate comfort days under the increasing climate comfort index (Yazdanpanah et al., 2016). A projection in China found that the heat-related excess mortality would increase from 1.9% in the 2010s to 2.4% in the 2030s and 5.5% in the 2090s under RCP8.5, and people with cardiorespiratory diseases, females, the elderly, and those with low educational attainment could be more affected (Yang et al., 2021). These findings pose great challenges to country policy-makers in designing safety mechanisms and protecting people working under continuous extreme hot weather conditions.

In areas with increasing population and economic density, and in which a larger amount of heat accumulates due to various anthropogenic factors, cities, and urban agglomerations are prone to the emergence of heat-related hazards (Geletič et al., 2020; J. Wang et al., 2021; Yao et al., 2022). For example, the heat island effect makes bioclimatic conditions more unfavorable in urban areas (Chen et al., 2020; Hou et al., 2021; Zhao et al., 2022). That is why the issue of summertime OTC in urban areas has become the subject of numerous studies (Milovanović, 2020). In addition, the effects of urbanization on nighttime temperature are more significant than that on daytime (Y. Sun et al., 2019; Zhou et al., 2004). Shi et al. (2021) found increased occurrence and severity of nighttime heat waves across China since 1980, and urbanization accounted for nearly 50% of the extended duration and nearly 40% of the enhanced intensity and frequency of nighttime heat waves in urban areas relative to rural areas. Consequently, more adverse effects of hot days may be aggravated by subsequent hot nights in urban areas. For instance, hot nights may be detrimental for restorative sleep following heat stress during daytime. Besides, the night economy is growing prosperous in urban areas in China, and people's nighttime outdoor activities are getting richer, especially in summer. People prefer to go out for entertainment or eat midnight snack at night, and some workers and farmers also try to work at night to avoid daytime heat. Sports enthusiast will even take midnight running in summer. Therefore, considering more adverse impacts on human health, the nighttime OTC that take into account nighttime relief needs more attention (Ma & Yuan, 2021; Shi et al., 2021; Wu et al., 2021).

Various indices have been proposed to evaluate the thermal stress levels. More than 100 simple thermal indicators have been developed over the last 150 years, and most of them are two-parameter indices. Such indices usually consist of air temperature and humidity combinations for warm conditions. For cold conditions, the combination typically consists of air temperature combined with airspeed (Jendritzky et al., 2012). Although simple indices are easy to calculate and forecast (Koppe et al., 2004), their results are often not comparable and have obvious regional limitations (Jendritzky et al., 2012). Since 1960, with the development of heat budget models (Gagge et al., 1986; Stolwijk, 1971), more comprehensive indices have been proposed, such as physiologically equivalent temperature (Mayer & Höppe, 1987), standard effective temperature (Gonzalez et al., 1974), predicted heat strain (ISO, 2004), and predicted mean vote (Fanger, 1970). These indices can, in principle, be appropriate for application in any assessment of the thermal environment. However, neither researchers nor end-users regard them as a fundamental standard, which may be related to the persistent shortcomings of thermal physiology and heat exchange theory (Jendritzky et al., 2012).

Since these indicators yet comprehensively consider bioclimatic conditions on human health, an integrated index including relevant meteorological parameters, such as air humidity, wind speed, and surface radiation, is needed (Jendritzky et al., 2008). An international committee was appointed to solve this problem, and the Universal Thermal Climate Index (UTCI) was developed based on long-term research (Jendritzky et al., 2002, 2012). UTCI is considered an indicator of organism thermal stress, which can objectively assess the impact of bioclimatic conditions on human organisms and compare research results in different climate regions (Błażejczyk et al., 2010). Since then, verifications and comparisons of UTCI have been carried out continuously, which has further verified the universal adaptability and superiority of UTCI (Asghari et al., 2019; Błażejczyk et al., 2014; Mohammadi et al., 2018; Zare et al., 2019). Compared to the present indicators, the UTCI represents specific climates, weather, and locations much better and preferably depicts the temporal variability of thermal conditions.

Furthermore, similar to the human body, the UTCI is very sensitive to changes in ambient stimuli, and its scale can express subtle differences in the intensity of meteorological stimuli (Blazejczyk et al., 2011).

Numerous studies that assessed the OTC based on thermal stress levels using the UTCI have been conducted in the past decade. Short-term OTC were widely assessed by UTCI. Bröde et al. (2012) defined optimal thermal comfort ranges for passers-by in pedestrian streets in southern Brazil, and suggesting that UTCI can serve as a suitable planning tool for urban thermal comfort in subtropical regions. J. Li et al. (2018) carried out a test including a physical measurement using UTCI and a questionnaire survey for OTC in Hong Kong in 2016, and found that the probability of these the desirability of sun and wind conditions for subjects fitted well with the UTCI in logistic regressions. Assessments were also carried out in Russia (Vinogradova, 2020), Algeria (Talhi et al., 2020), Iran (Asghari et al., 2019; Baaghideh et al., 2016; Mohammadi et al., 2018), and several European countries, such as Poland (Błażejczyk et al., 2014; Okoniewska, 2020) and Serbia (Milovanović, 2020; Pecelj et al., 2020). To the best of our knowledge, there is still a lack of a method to evaluate the regional OTC that considers long-term bioclimatic conditions based on the UTCI assessment.

The applications of UTCI and the assessment of OTC still face some problems. While past studies focused on either the national scale or the fine scale (e.g., urban streets), there are few UTCI distribution maps at regional scales, such as urban agglomerations. In addition, UTCI characterizes thermal stress in humans caused by ambient conditions, but several researchers use UTCI directly for OTC assessment, which may be unsuitable and inconvenient for long-term analysis and regional comparisons (Blazejczyk, 2021). In addition, evaluating the regional OTC should also consider the intensity, duration, and extent of thermal stress, which is similar to assessing heatwave events.

Therefore, this study focused on the summertime OTC in urban agglomerations and selected China's Beijing-Tianjin-Hebei (BTH) urban agglomeration as the study area. To describe the long-term OTCs of regions and better for comparisons, a summarized score, the Composite Thermal Comfort Score (CTCS), was proposed. CTCS takes into account the extent, duration, and intensity of the thermal stress assessed by the UTCI, which could comprehensively evaluate the OTC of cities. Furthermore, considering the increasing heat island effect and nighttime heatwaves, both daytime UTCI and nighttime UTCI were used to analyze and assess OTC at day and night during the past 40 years (1981–2020), respectively. This study revealed the spatiotemporal pattern and trend of the UTCI, frequencies of each thermal stress level, and OTC of cities in BTH.

2. Materials and Methods

2.1. Study Area

BTH is located in North China (Figure 1), including Beijing municipality (the capital and second-largest city of China), Tianjin municipality, and Hebei province. It borders the Yanshan Mountain in the north, North China Plain in the south, Taihang Mountain in the west, and Bohai Bay in the east. The structure of the Yanshan-Taihang mountain system from northwest to southeast gradually transitions into a plain, showing topographic characteristics of high in the northwest and low in the southeast. Consequently, BTH can be divided into three parts for analysis: the northern mountainous zone (Zhangjiakou and Chengde), the mountain-plain transition zone (Beijing, Tangshan, and Qinhuangdao), and the southern plain zone (Shijiazhuang, Xingtai, Handan, Baoding, Langfang, Cangzhou, and Hengshui).

As one of China's three vast urban agglomerations, BTH has experienced rapid urbanization and a high concentration of population and economy. The gross domestic product of BTH in 2020 totaled 8.5 trillion-yuan, accounting for 8.5% of the country. Additionally, it has become one of the vital population inflow places in China due to its superior economic conditions and employment environment. From 2008 to 2018, the population increments of BTH were 3.832, 3.836, and 5.673 million, respectively, and the population growth rates were 20.6%, 31.2%, and 8.1%, respectively (Chen, 2019).

Since the 1960s, the average annual temperature in the BTH has shown a significant increasing trend, and the warming rate varies, generally ranging from 0.29°C/10a to 0.34°C/10a (Qin et al., 2021; Si et al., 2021; Zhe et al., 2020), which is higher than the national average in the same period. The climate warming is even accelerating after the 1990s (P. F. Li et al., 2015; W. J. Zhang et al., 2021). Meanwhile, previous studies also have shown

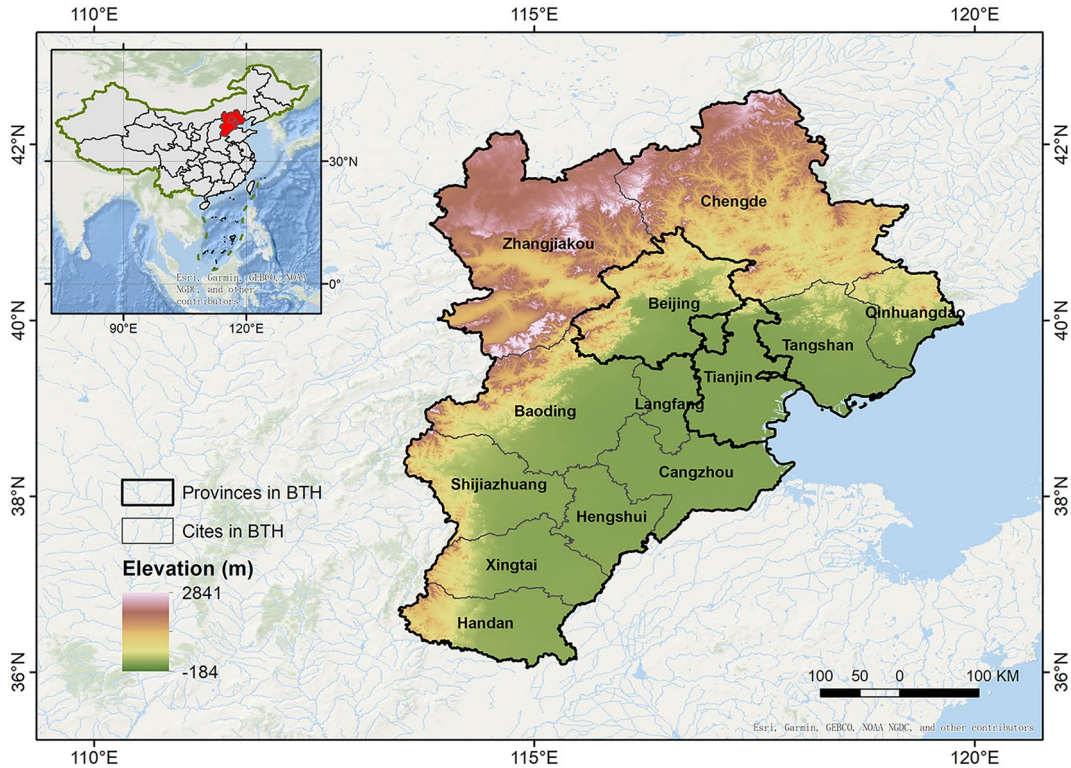

Figure 1. Location of the Beijing-Tianjin-Hebei urban agglomeration.

that the UHI intensity in the BTH is increasing significantly at a rate of 1.0°C/10a, and the spatial extent is rapidly increasing, expanding and connecting, gradually forming a large UHI agglomeration area (Liu et al., 2020).

2.2. The Research Framework

Figure 2 presents the framework of this study, ranging from the grid to the region. Meteorological variables for UTCI calculation were first derived from ERA5_Land and ERA5 data sets. After data preprocessing (Section 2.3), a high-spatial-resolution data set of daily UTCI in the summer from 1981 to 2020 was obtained using the UTCI

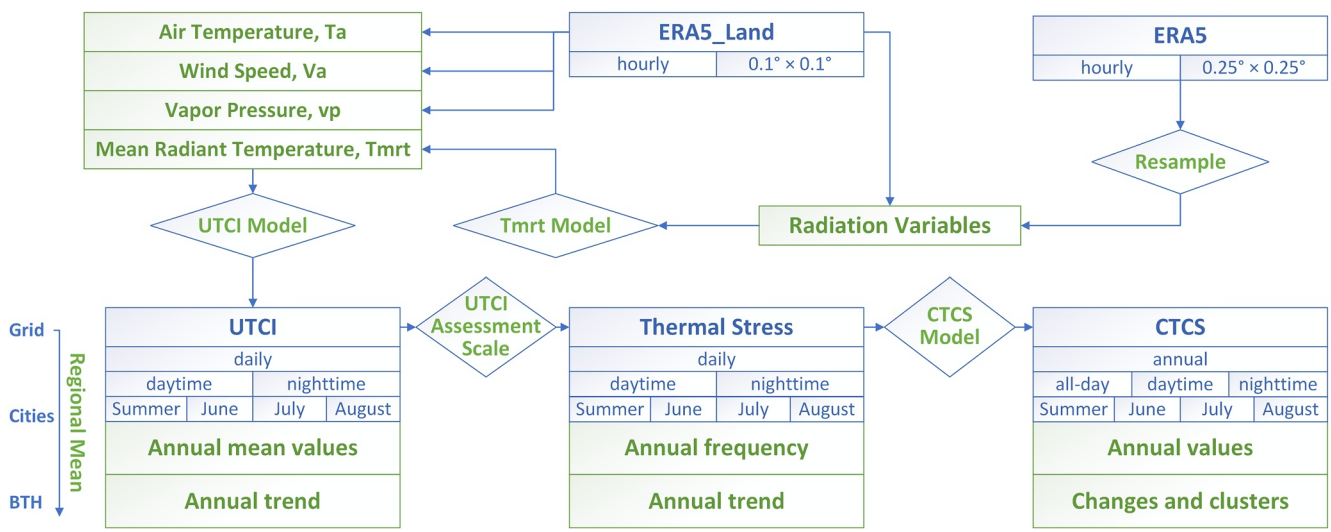

Figure 2. The framework of the study.

Table 1
Variables From ERA5-Land and ERA5 for Universal Thermal Climate Index

Variable	Description	Units	Source data set
T_a	The air temperature at 2 m above the ground	K	ERA5-Land
T_d	Dewpoint temperature at 2 m above the ground	K	ERA5-Land
u	Eastward component of the 10 m wind	m s^{-1}	ERA5-Land
v	Northward component of the 10 m wind	m s^{-1}	ERA5-Land
ssrd	Surface solar radiation downward: the amount of shortwave radiation that reaches a horizontal plane at the surface	J m^{-2}	ERA5-Land
ssr	Surface net solar radiation: the amount of shortwave radiation that reaches a horizontal plane at the surface minus the amount reflected at the surface	J m^{-2}	ERA5-Land
strd	Surface thermal radiation downward: the amount of longwave radiation emitted by the atmosphere and clouds that reaches a horizontal plane at the surface	J m^{-2}	ERA5-Land
str	Surface net thermal radiation: the difference between downward and upward longwave radiation passing through a horizontal plane at the surface	J m^{-2}	ERA5-Land
fdir	Direct solar radiation at the surface: the amount of direct shortwave radiation passing through a horizontal plane at the Earth's surface	J m^{-2}	ERA5

model (Section 2.4). Then, based on the UTCI assessment scale (Section 2.5), the UTCI values are categorized into 10 levels of thermal stress, from extreme cold stress (ECS) to EHS. Finally, the CTCS of each city was calculated according to the regional-averaged frequencies of thermal stress categories over years. Since the CTCS integrate the frequencies of each thermal stress levels across the region within a period of time, it could comprehensively reflect the intensity, duration, and extent of thermal stress (Section 2.6).

The annual mean values and trend of UTCI, the annual frequency and trend of thermal stress categories, and the annual values and changes of CTCS in regions were analyzed (Section 2.7). In the temporal dimension, the daily UTCI includes two indicators of daytime and nighttime. The annual UTCI was averaged by daily UTCI in every summer and its corresponding 3 months (June–August), and then the trend of annual UTCI was analyzed. The process of thermal stress and CTCS series are similar to the UTCI series, while the CTCS was obtained on annual scale and contain three indicators of daytime, nighttime, and all-day. In the spatial dimension, the grid scale was first obtained and the regional scale (city and BTH) data was calculated based on grid data using zoning statistics (mean) through the administrative boundaries of regions.

2.3. Data and Preprocessing

The details of the variables used for UTCI calculation in this study are shown in Table 1. A set of meteorological data, including air temperature and humidity, wind speed, and shortwave and longwave radiation fluxes, are derived from the ERA5 (Hersbach et al., 2018) and ERA5-Land (Muñoz Sabater, 2019) data sets since they provide complete high-resolution meteorological variables for UTCI calculation (Di Napoli, Barnard, et al., 2020; Di Napoli, Hogan, & Pappenberger, 2020). These gridded data sets have been applied to compute the UTCI at global and regional scales and verified its effects in China (Yan et al., 2021). Hourly meteorological variables were retrieved from ERA5-Land, except for the direct solar radiation (fdir), which is available only in ERA5 with a coarser resolution. fdir is resampled from 0.25° resolution to 0.1° using nearest-neighbor interpolation to match the other variables. Furthermore, the accumulated radiation values (J m^{-2}, as in Table 1) in the original ERA5-Land and ERA5 datasets are transformed to hourly values (ECMWF, 2019; Muñoz Sabater, 2019).

2.4. UTCI Model

UTCI is defined as the "equivalent temperature for a given combination of wind speed, radiation, humidity, and air temperature as the air temperature of the reference environment which produces the same strain index value" (Jendritzky et al., 2012). It is based on an advanced human thermal balance model, that is, the UTCI-Fiala multinode model (Fiala et al., 2012), coupled with the adaptive clothing model (Havenith et al., 2012). This study

calculated the hourly deviation of the mean radiant temperature (Tmrt) and UTCI from 1981 to 2020 in BTH based on the ERA5-Land and ERA5 reanalysis products according to the proposed approach by Yan et al. (2021).

The offsets of UTCI to air temperature (T_a, K) are approximated by a polynomial in T_a, wind speed (V_a, m/s), humidity expressed as water vapor pressure (vp, hPa), and the difference between Tmrt and T_a, including all the main effect and interaction terms up to the 6-order (Jendritzky et al., 2008). This process can be expressed as the following function (Equation 1):

$$\mathrm{UTCI} = f(T_a,\ V_a, \mathrm{vp}, \mathrm{Tmrt}) = Ta + \mathrm{Offset}(T_a, V_a, \mathrm{vp},\ \mathrm{Tmrt} - T_a) \tag{1}$$

The V_a can be calculated from eastward component u and northward component v as follows:

$$V_a = \sqrt{u^2 + v^2} \tag{2}$$

The vp is calculated from dewpoint temperature T_d as follows:

$$\mathrm{vp} = 6.11 \times \mathrm{e}^{5417.753\times(1/273.16-1/T_d)} \tag{3}$$

Tmrt is the critical component of UTCI, defined as "the temperature of an imaginary isothermal black enclosure in which a solid body or occupant would exchange the same amount of heat by radiation as in the actual nonuniform enclosure" (Gonzalez et al., 1974). The value is shaped by streams of shortwave and longwave radiation reaching the body. The calculation of Tmrt is often complex and requires several procedures (Blazejczyk, 2001; Di Napoli, Barnard, et al., 2020; Di Napoli, Hogan, & Pappenberger, 2020; Matzarakis et al., 2007; Thorsson et al., 2007). A widely accepted method to calculate Tmrt for the outdoor environment was given (Equation 4) by Weihs et al. (2012).

$$\mathrm{Tmrt} = \sqrt[4]{\frac{1}{\sigma} \times \left[\frac{\alpha_k}{\varepsilon_p} \times (f_p \times I_{\mathrm{sw}} + f_a \times D_{\mathrm{sw}} + f_a \times R_{\mathrm{sw}}) + f_a \times (D_{\mathrm{lw}} + U_{\mathrm{lw}})\right]} - 273.5 \tag{4}$$

where σ is the Stefan Boltzmann constant (5.67×10^{-8} W m^{-2} K^{-4}), α_k is the absorption coefficient of the typical human body for shortwave radiation (standard value 0.7), and ε_p is the emissivity coefficient of the human body (standard value 0.97), f_a is the solid angles and set to 0.5, f_p is the projected area factor, which accounts for the directional dependence and is a function of the solar zenith angle (Equation 5) (Jendritzky et al., 1990; Leroyer et al., 2018). I_{sw}, D_{sw}, R_{sw}, D_{lw}, and U_{lw} are the anisotropic incident direct shortwave radiation flux, isotropic diffuse shortwave radiation flux, the surface reflected shortwave radiation flux, downwelling longwave radiation fluxes, and upwelling longwave radiation fluxes, respectively, all expressed in W m^{-2} and were calculated from the accumulated radiation values in the original data set, as shown in Equations 6–10 (Yan et al., 2021).

$$f_p = 0.308 \times \cos\left\{\left(\frac{\pi}{2} - \theta\right) \times \left[1 - \frac{\left(90 - \frac{180}{\pi}\theta\right)^2}{48402}\right]\right\} \tag{5}$$

$$I_{\mathrm{sw}} = \mathrm{fdir}/\cos\theta/3600 \tag{6}$$

$$D_{\mathrm{sw}} = (\mathrm{ssrd} - \mathrm{fdir})/3600 \tag{7}$$

$$R_{\mathrm{sw}} = (\mathrm{ssrd} - \mathrm{ssr})/3600 \tag{8}$$

$$D_{\mathrm{lw}} = (\mathrm{strd} - \mathrm{str})/3600 \tag{9}$$

$$U_{\mathrm{lw}} = \mathrm{strd}/3600 \tag{10}$$

where θ is the solar zenith angle (in radians), the cosine of θ can be calculated following as Equation 11 (Woan, 2000):

$$\cos\theta = \sin\delta \sin\varphi + \cos\delta \cos\varphi \cos h \tag{11}$$

Table 2
Thermal Stress Categories and Corresponding Protection Measures

UTCI (°C)	Stress categories (Błażejczyk et al., 2013)	Protection measures (Krzyżewska et al., 2020)
<−40	Extreme cold stress (ECS)	Stay indoors or use heavy and wind-protected clothing
−40~−27	Very strong cold stress (VSCS)	Strongly increase activity, protect face and extremities; use better-insulated clothing and reduce stay outdoor
−27~−13	Strong cold stress (SCS)	Strongly increase activity, protect face and extremities; use better-insulated clothing
−13~0	Moderate cold stress (MCS)	Increase activity, and protect extremities and face against cooling
0~9	Slight cold stress (SICS)	Use gloves and caps
9~26	No thermal stress (NTS)	Physiological thermoregulation sufficient to keep comfort
26~32	Moderate heat stress (MHS)	Drinking >0.25 $L \cdot h^{-1}$ necessary
32~38	Strong heat stress (SHS)	Drinking >0.25 $L \cdot h^{-1}$ necessary. Use shade places and reduce activity
38~46	Very strong heat stress (VSHS)	Periodical use of air conditioning or shaded sites and drinking >0.5 $L \cdot h^{-1}$ necessary; reduce activity
>46	Extreme heat stress (EHS)	Periodical cooling and drinking >0.5 $L \cdot h^{-1}$ necessary; stay without activity

where φ is the geographical latitude, δ is the solar declination angle as a function of a given date of the year and h is the hour angle in local solar time. The latter two parameters, that is, δ and h, are calculated following Spencer (1971) and NOAA (NOAA, 1997).

2.5. UTCI Assessment Scale

The daily maximum and minimum values of UTCI were selected as daytime UTCI and nighttime UTCI, respectively. The UTCI values were categorized in terms of thermal stress levels and corresponding protection measures, as Table 2 provides. The UTCI assessment scale were proposed when UTCI model developed publicly. It looks at responses to reference conditions and deducts the thermal load (i.e., the heat or cold stress) caused by the organism's physiological response to actual environmental conditions (Błażejczyk et al., 2013). It shows an asymmetric distribution with more categories on the cold side, which may partly reflect the sensitivity of the UTCI model to wind speed (Brode et al., 2012).

Meanwhile, based on the UTCI assessment scale, previous studies had demonstrated the potential of UTCI as a bioclimatic index that is able to both capture the thermal bioclimatic variability, and related health risk on human. Di Napoli et al. (2018) revealed that the relationship between the UTCI and death counts depends on the regional bioclimate in 17 European countries, and death counts increase in conditions of moderate stress and strong stress. A long-term, multi-city study in Poland also found that the relative risk (RR) of death rose by 10%–20% in most of the cities in strong stress conditions, and RR rose to 25%–30% in central Poland in very strong stress conditions (Kuchcik, 2020). Hence, this study used the UTCI assessment scale to categorize thermal stress level based on the daytime and nighttime UTCI to capture the regional bioclimatic variability and related health risk.

2.6. Composite Thermal Comfort Score (CTCS) Model

OTC refers to bioclimatic conditions suitable for most people. While UTCI is applicable to characterize thermal stress in humans caused by ambient conditions, it can only give instructions for a particular time and place. To assess the overall OTC of a region over time and compare the OTC performance between regions, a sophisticated score is needed to integrate the thermal stress that is characterized by the UTCI in each period for an area.

Therefore, this study proposed a CTCS as the integrated assessment of regional OTCs. Due to limited studies on the comfort scale definition using UTCI, we refer to the categories and scoring of the comfort of human body index (ICHB). This method is defined by the China Meteorological Administration and widely used in studies in China (Lei et al., 2020; G. Sun et al., 2011). As shown in Table 3, each stress category was first mapped to a comfort weight. No thermal stress (NTS) was mapped to 1 since it is regarded as the condition of comfort, and

Table 3
Comfort Weights of Stress Categories for Outdoor Thermal Comfort

ID	Stress categories	Comfort weights
0	Extreme cold stress (ECS)	−4
1	Very strong cold stress (VSCS)	−3
2	Strong cold stress (SCS)	−2
3	Moderate cold stress (MCS)	−1
4	Slight cold stress (SICS)	0
5	No thermal stress (NTS)	1
6	Moderate heat stress (MHS)	−1
7	Strong heat stress (SHS)	−2
8	Very strong heat stress (VSHS)	−3
9	Extreme heat stress (EHS)	−4

heat/cold stress categories from moderate level to extreme level were mapped from −1 to −4. The one extra category with slight cold stress (SICS) was mapped to 0.

Then, the CTCS could be defined as the weighted frequencies of stress categories occurring over a period and averaged in a region, as shown in Equation 12.

$$\mathrm{CTCS} = \frac{\sum_{i=1}^{n}\sum_{j=0}^{9}(q_{ij} \times w_j)}{n} \tag{12}$$

where n is the total number of grids in a region (i.e., the grid number in BTH is 2211), i is the ith grid in the region, j is the ID of thermal stress categories, q_{ij} refers to the frequency of thermal stress j occurring in grid i over a period, and w_j refers to the comfort scale regarding the thermal stress category j.

Since the stress categories evaluate the intensity of thermal stress, the frequencies of stress categories consider the duration of thermal stress, and the regional averages reflect the extent of thermal stress. The CTCS could well evaluate regional OTC by integrating the intensity, duration, and extent of thermal stress.

In this study, based on the calculated daytime UTCI and nighttime UTCI, the annual occurrence percentage of thermal stress categories at the grid scale were first evaluated, and then the daytime CTCS and nighttime CTCS could be calculated from 1981 to 2020 using Equation 12 proposed above. Additionally, all-day CTCS could be defined as the sum of daytime CTCS and nighttime CTCS, referring to the overall OTC condition in the whole day, as shown in Equation 13.

$$\mathrm{CTCS}_{\text{all-day}} = \mathrm{CTCS}_{\text{daytime}} + \mathrm{CTCS}_{\text{nighttime}} \tag{13}$$

To assess and compare the overall comfortable conditions across the cities in BTH cities should be classified into several groups based on values and variations of the annual daytime, nighttime, and all-day CTCS series. To make the classification more reliable, a cluster analysis of the annual CTCS series was first derived to identified the groups of cities with similar CTCS both in values and variations. The K-Means clustering method and the Dynamic Time Warping distance were used to calculate the distances between time series since it better considered and measured the similarity of time series (Müller, 2007). Cities would be classified into the four groups in order of averaged CTCS from high to low using Natural Breaks method in ArcGIS, representing the relative comfortable conditions from comfortable to uncomfortable in BTH compared to the other cities.

It is worth noting that compared with the UTCI as a thermal indicator based on the human thermal balance model that characterizes thermal stress, CTCS is better described as a comprehensive, summarized score for regional OTC that takes into account the extent, duration, and intensity of daily thermal stress cross an extended period. Hence, UTCI could be used to describe the local bioclimatic conditions, and the CTCS needs to consider the spatiotemporal scale before comparison and analysis since their principle of them are different.

2.7. Time-Series Analysis Method

The annual trends of UTCI and thermal stress frequencies of BTH and cities were analyzed by the Mann–Kendall (Kendall, 1975; Mann, 1945) and the Sen's slope (Sen, 1968) tests. They have the advantage of not require any special form of assumptions on the data distribution functions, while having powers almost as high as their parametric competitors, and they were highly recommended by the World Meteorological Organization (Mourato et al., 2010; Nalley et al., 2013).

In addition, considering that the annual thermal stress frequencies are "compositional," that is, they sum up to 100%, and are thus inherently negatively correlated (i.e., an increase in one category has to be accompanied by a decrease in other categories). Hence, we assign one category (e.g., moderate heat stress [MHS]/NTS) as reference, and to consider the ratios of other thermal stress to the reference, and how they change over time. Since the reference could not be zero, for daytime series, we selected MHS category as reference, and selected NTS

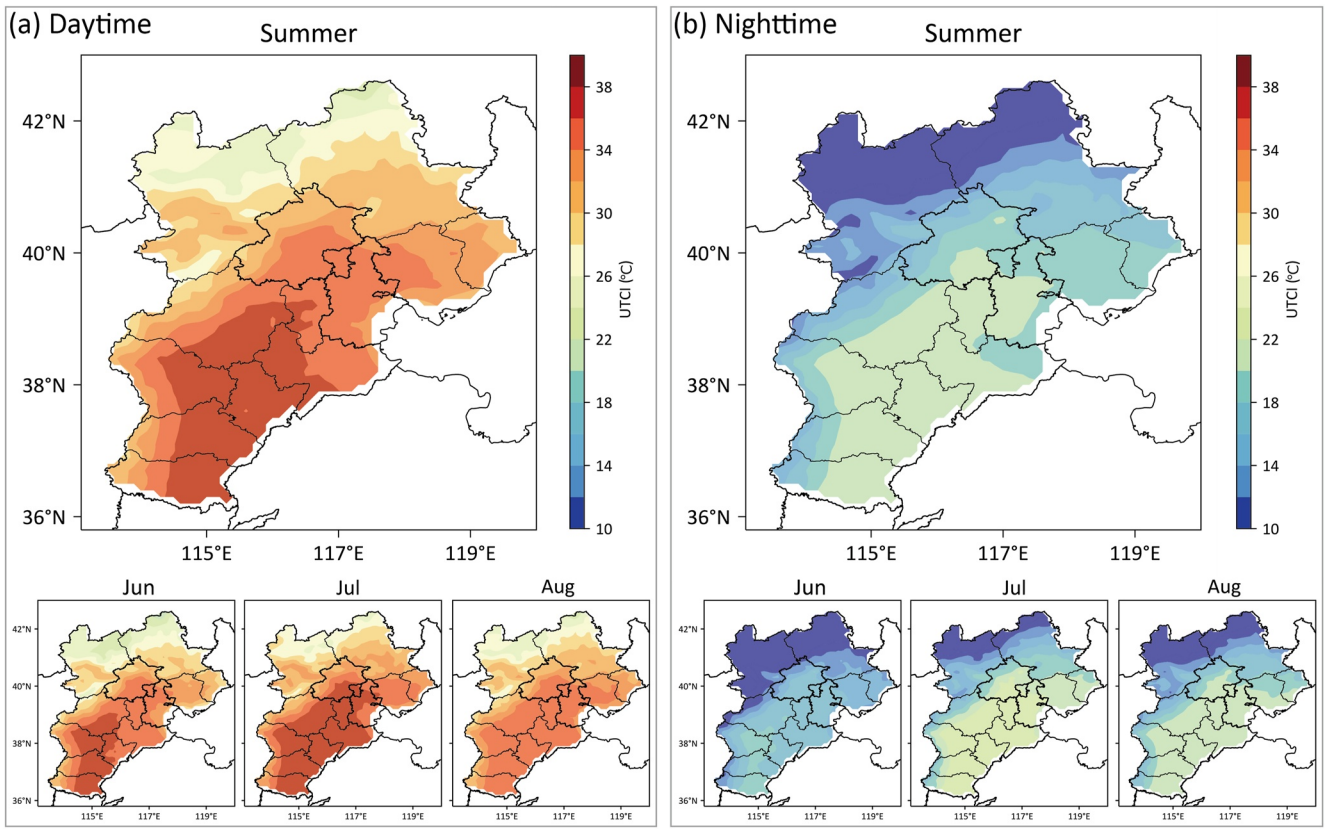

Figure 3. Maps of the averaged (a) daytime Universal Thermal Climate Index (UTCI) and (b) nighttime UTCI in Beijing-Tianjin-Hebei.

category as reference for nighttime series. The trends of ratios were also analyzed by the Mann–Kendall and the Sen's slope tests.

3. Results

During the investigated period (1981–2020), we first analyzed the spatiotemporal patterns and changes in UTCI and thermal stress for the overall BTH. Then, comparisons and discussions of UTCI and thermal stress at the city scale were carried out. Finally, the overall conditions and changes in OTC for cities in BTH were evaluated using the proposed CTCS model.

3.1. UTCI and Thermal Stress in the BTH

Figure 3 shows the averaged UTCI maps in summer, June–August during daytime (Figure 3a) and nighttime (Figure 3b) over BTH. The spatial pattern of the UTCI distinctly showed a general gradient from north to south and from high altitude to low altitude. Consequently, BTH can be divided into three parts: the northern mountainous zone (Zhangjiakou and Chengde), the mountain-plain transition zone (Beijing, Tangshan, and Qinhuangdao), and the southern plain zone (Shijiazhuang, Xingtai, Handan, Baoding, Langfang, Cangzhou, and Hengshui).

For the daytime, the averaged UTCI in BTH in summer is 32°C and that in July is up to 33°C (reaching the strong heat stress [SHS]). Most areas in BTH suffer heat stress, with averaged UTCIs larger than 26°C, except for small parts in the northern mountainous zone. The averaged UTCIs of the mountain-plain transition zone range from 26°C to 38°C. However, the southern plain zone totally experiences SHS in summer, with averaged UTCIs greater than 32°C. July is when the area of the averaged UTCI is more than 36°C and expands significantly. The spatial pattern of the averaged nighttime UTCI in BTH is similar to that during the daytime, yet the intensities are not. The averaged nighttime UTCI is 16°C in summer and down to 13°C (reaching the NTS) in June. All averaged nighttime UTCIs are between 9°C and 26°C, which are much lower and indicate that BTH has NTS on the

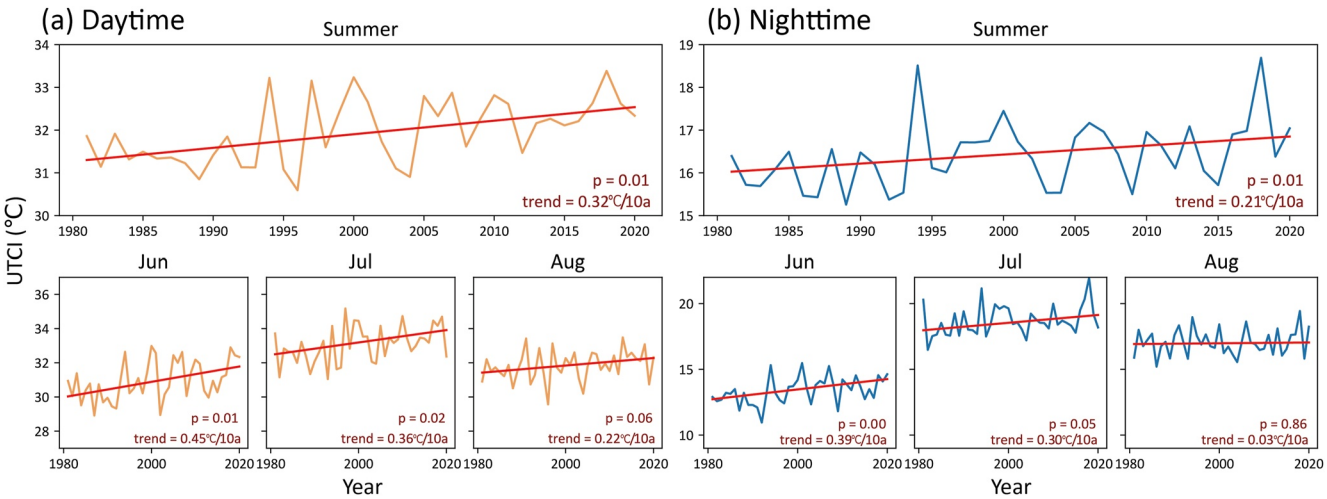

Figure 4. Temporal changes in the annual mean (a) daytime Universal Thermal Climate Index (UTCI) and (b) nighttime UTCI in Beijing-Tianjin-Hebei.

summer nights on average. However, it should be noted that the averaged nighttime UTCIs in the southern plain zone primarily range between 24°C and 26°C in July, reaching the boundary of the MHS.

Figure 4 presents the temporal change and trend of the annual mean daytime UTCI and nighttime UTCI in summer, June–August in BTH. The red lines indicate the trend of the annual mean UTCI. The daytime UTCI in summer shows a rising fluctuation trend with an increasing rate of 0.32°C/10a. The increasing rates in June (0.45°C/10a) and July (0.36°C/10a) are significantly higher than those in August (0.22°C/10a). The nighttime UTCI also shows an increasing trend with a rate of 0.21°C/10a. June has the greatest nighttime warming trend, with an increasing rate of 0.39°C/10a.

Figure 5 depicts the averaged occurrence percentage of thermal stress categories during daytime and nighttime in BTH. Obviously, during the day, the BTH experiences more MHS (36%) and SHS (42%) conditions in summer. In addition, very strong heat stress (VSHS) (10%) conditions are also frequent, especially in July (14%). In contrast, NTS conditions are prevalent (85%) at night. Cold stress (1% in moderate cold stress [MCS] and 11% in SICS) even occurred more frequently than heat stress (3% in MHS), especially in June (20% cold stress and no heat stress).

Figure 6 shows the annual trend of thermal stress categories during daytime and nighttime in summer, June–August in BTH. At summer daytime, although days in MHS decreased by 1.31 d/10a, VSHS and SHS days significantly increased by 0.64 and 1.56 d/10a, and on the whole heat stress days increased by 0.88 d/10a, indicating more frequency and intensity of heat stress in BTH in recent years. At nighttime, cold stress days decreased, and NTS and MHS days increased in summer (0.21 and 0.39 d/10a, respectively). From the view of months, more NTS days in June increase significantly by 0.49 d/10a, indicating that the bioclimatic conditions are becoming

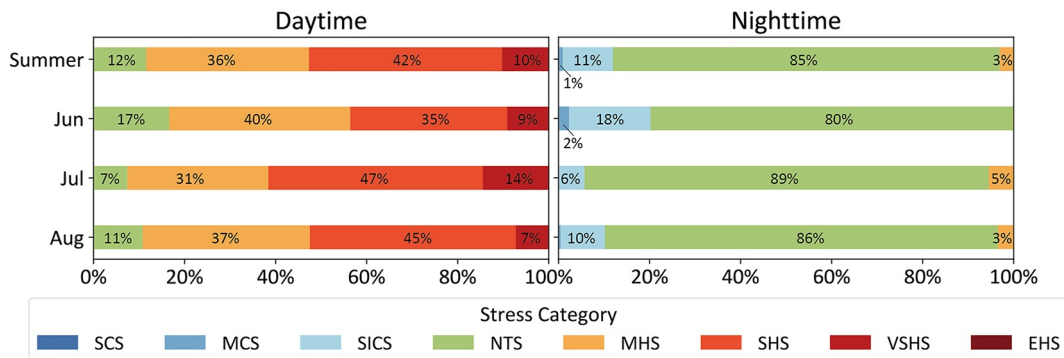

Figure 5. Averaged frequencies of thermal stress categories during daytime and nighttime in Beijing-Tianjin-Hebei.

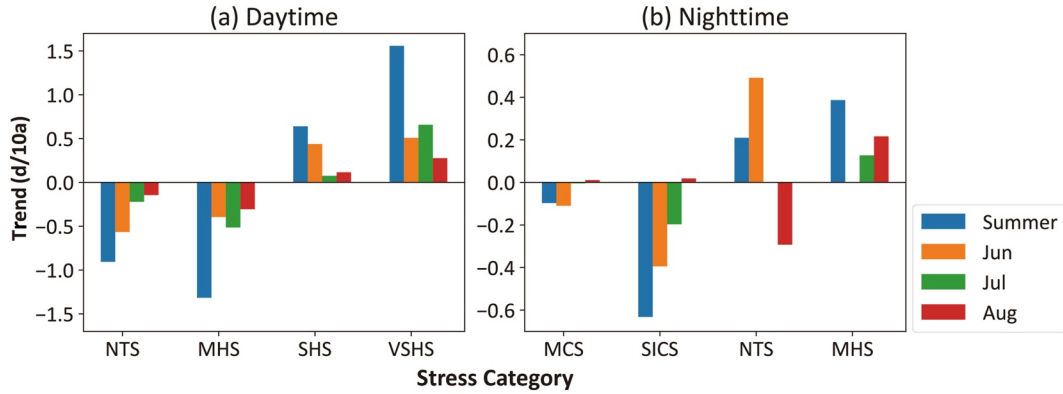

Figure 6. Annual trends (in days) of thermal stress categories at (a) daytime and (b) nighttime in Beijing-Tianjin-Hebei.

more favorable. In August, NTS days decreased by 0.30, and MHS days increased by 0.22 d/10a, representing a more unfavorable bioclimatic condition. Figure S1 in Supporting Information S1 shows the annual trends (in times) of frequency ratios of thermal stress to MHS at daytime and NTS at nighttime in BTH. It further confirms that results of Figure 6. At summer daytime, compare to the MHS, VSHS, and SHS greatly increased and highest in July, NTS decreased and highest in June. At nighttime, MHS increased and highest in August, cold stress generally decreased and highest in June.

3.2. UTCI and Thermal Stress at the City Scale

Figure 7 shows the averaged daytime UTCI and nighttime UTCI in the summer of the cities in BTH. For the summer daytime, all cities except Zhangjiakou and Chengde have a UTCI of more than 32°C and reach the heat stress of SHS. July has a higher UTCI, and the temperature difference between July and June is up to 1°C–3°C. Great differences exist between cities and follow the increasing gradient of UTCI from north to south and from high altitude to the low. Zhangjiakou and Chengde (the northern mountainous zone) have the lowest UTCI (27.9°C and 28.6°C, respectively), all cities located in the southern plain zone have a UTCI greater than 34°C, and Hengshui has the highest (36.3°C). For summer nighttime, the UTCI in cities ranges from 9°C to 26°C

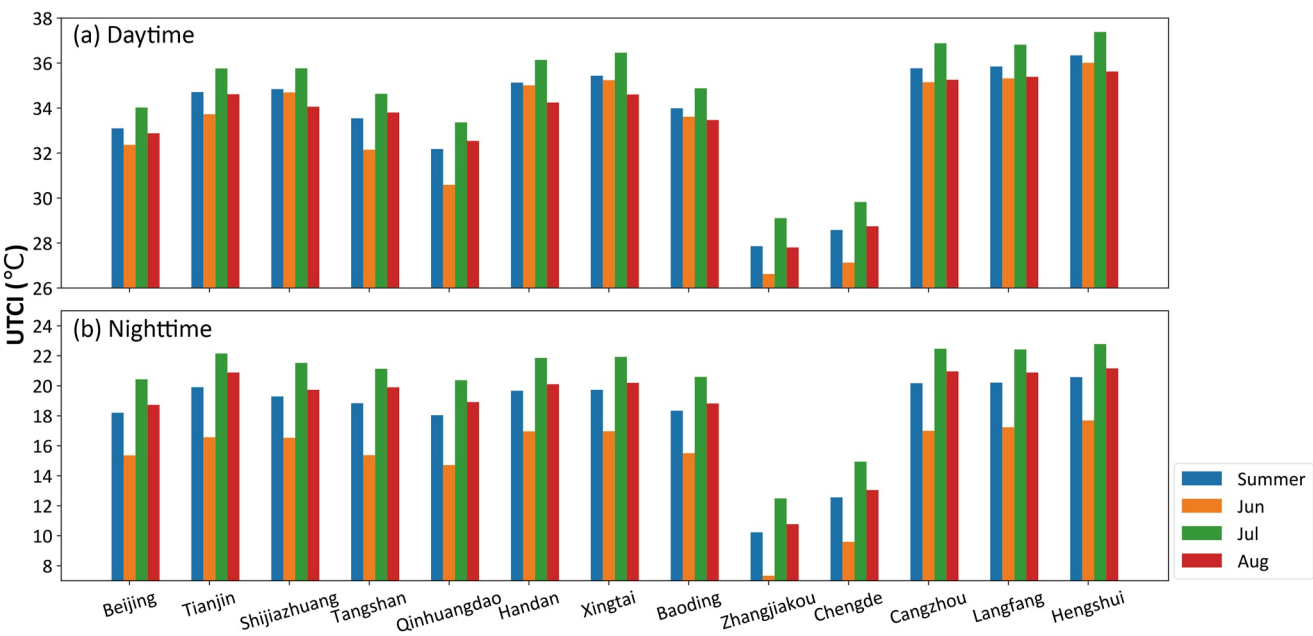

Figure 7. Averaged (a) daytime Universal Thermal Climate Index (UTCI) and (b) nighttime UTCI of cities in Beijing-Tianjin-Hebei.

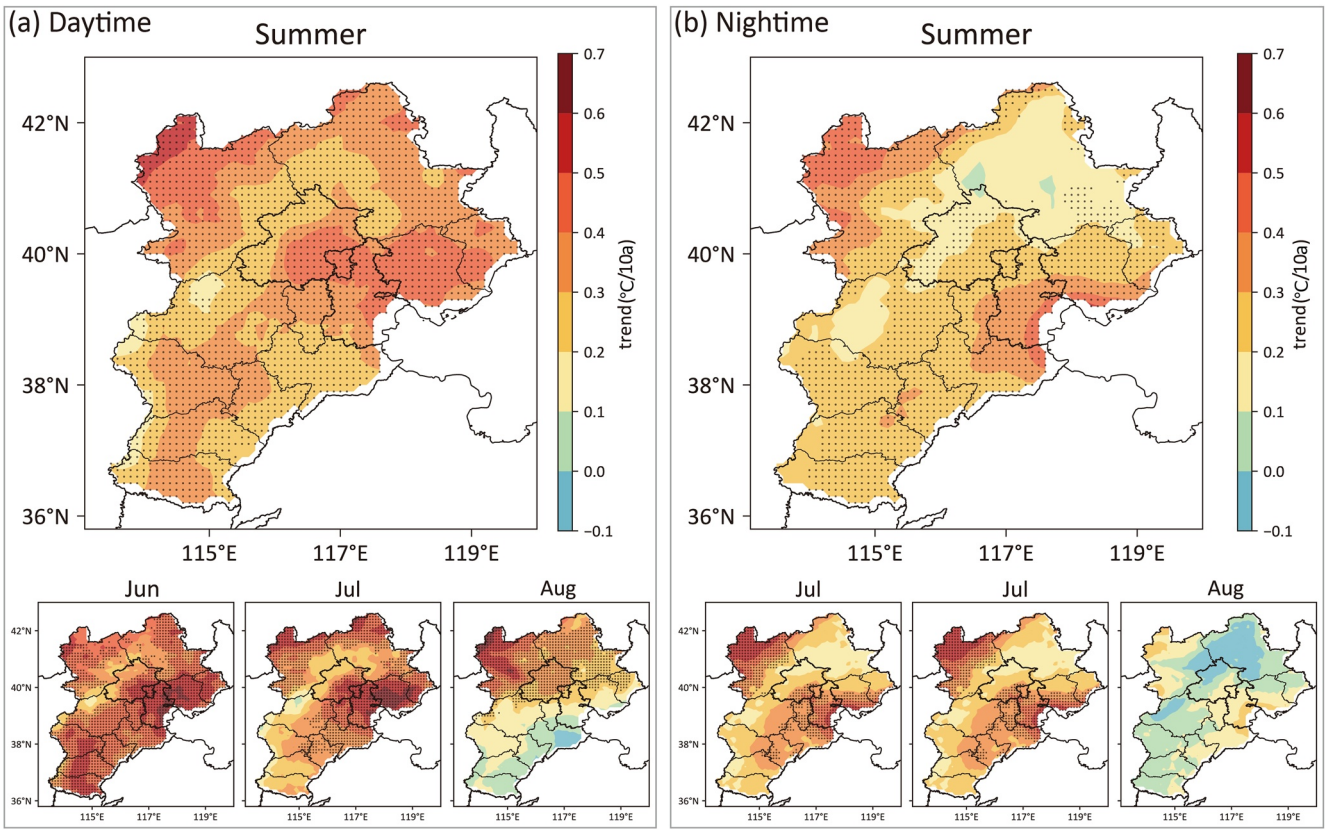

Figure 8. Maps of annual trends of (a) daytime Universal Thermal Climate Index (UTCI) and (b) nighttime UTCI in Beijing-Tianjin-Hebei (black dots indicate the significance level at 0.05).

(reaching the NTS), indicating generally comfortable conditions. June in Zhangjiakou is not comfortable since the UTCI is as low as 7.3°C (reaching the SICS). June is the coolest month, and the temperature difference between July and June is up to 4°C–6°C.

Figure 8 shows the annual trends of daytime and nighttime UTCI in BTH. The black dots indicate significance at the 0.05 level. The spatial pattern of the UTCI trends differs from that of the UTCI values. The summer daytime UTCIs present a significantly increasing trend over the region, whereas the areas with large rising rates (>0.4°C/10a) are concentrated in Beijing, Tianjin, Tangshan, and Zhangjiakou. In months, areas with high increasing rates (>0.5°C/10a) in June are mainly northwest of Zhangjiakou and adjacent to Bohai Bay. The high-increasing areas (>0.5°C/10a) expanded to Beijing, Tianjin, and Tangshan in July. In August, the areas concentrated to the northwest of Zhangjiakou have a higher increase rate (>0.5°C/10a) than other areas. At nighttime, the high-increasing areas with more than 0.3°C/10a are distributed mainly in the northwest mountainous Zhangjiakou regions and the coastal zones adjacent to Bohai Bay. In terms of months, the increasing rates of nighttime UTCIs in June are higher than those in daytime, and two major high rates (>0.5°C/10a) clusters are located in Beijing, Tianjin, and Tangshan as well as in Shijiazhuang, Xingtai, and Handan. Areas with large increasing rates (>0.4°C/10a) in July are mainly northwest of Zhangjiakou and adjacent to Bohai Bay.

Furthermore, Figure 9 provides the daytime and nighttime UTCI trends of cities in BTH. The daytime UTCI shows an increasing trend in summer and each month. Generally, the increase rates in June and July were higher than those in August and the whole summer. For instance, Tianjin, Tangshan, and Langfang have the top three rates in June (0.56°C/10a, 0.57°C/10a, and 0.49°C/10a, respectively) and July (0.54°C/10a, 0.57°C/10a, and 0.48°C/10a, respectively). Surprisingly, the increasing rate of daytime UTCI in August in Zhangjiakou (0.46°C/10a) was the highest over BTH. For the nighttime UTCI, all cities show increasing trends in summer, yet the rates were lower than those in the daytime. Trends were higher in June and lower in August. Chengde even shows a decreasing

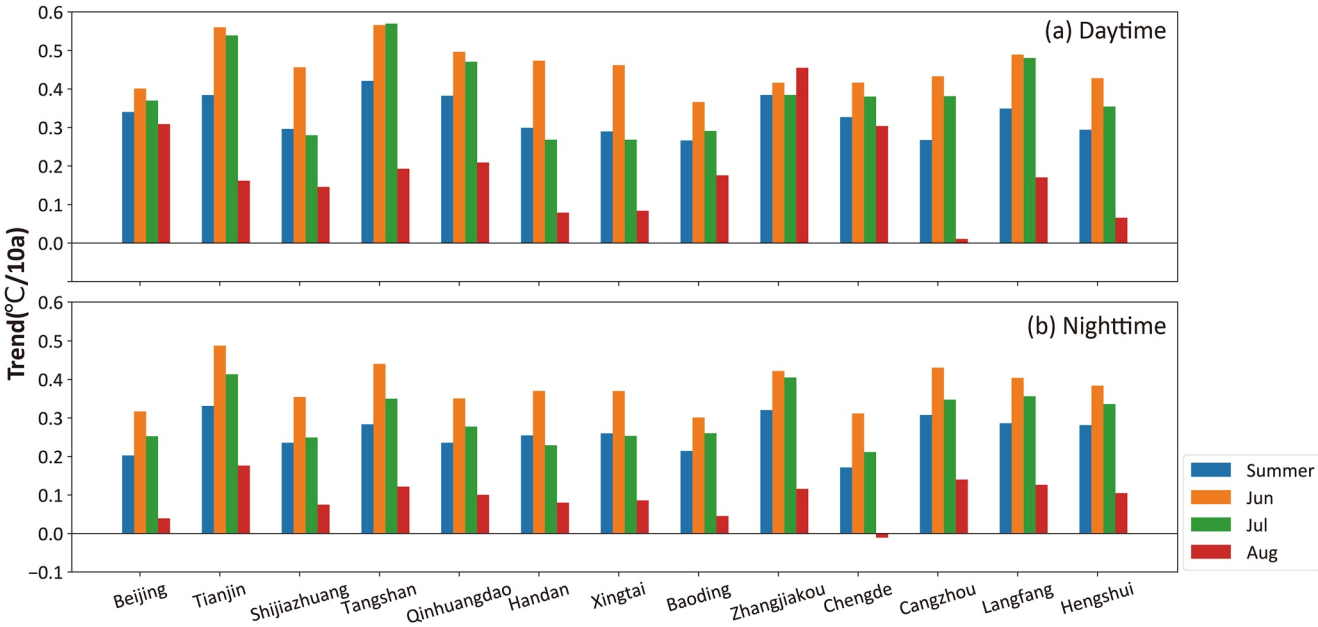

Figure 9. Averaged trends of (a) daytime Universal Thermal Climate Index (UTCI) and (b) nighttime UTCI of cities in Beijing-Tianjin-Hebei.

trend in August. Coastal and mountainous cities, for example, Tianjin, Tangshan, Cangzhou, and Zhangjiakou, had higher rates, especially in June (0.49°C/10a, 0.44°C/10a, 0.43°C/10a, and 0.42°C/10a, respectively).

We also explored the annual frequencies and trends of the thermal stress categories at the city scale. Figure 10 shows the frequencies of thermal stress categories of cities in BTH both at daytime and nighttime. Maps of frequencies can be seen in Figures S2 and S3 in Supporting Information S1, and a similar gradient pattern from north to south can be found. At daytime, more NTS and MHS occurred in the northern mountainous zone; for instance, Zhangjiakou and Chengde have the highest frequencies of NTS (30% and 24%, respectively) and MHS (52% and 53%, respectively) over BTH without VSHS days, presenting the most favorable bioclimatic conditions. The mountain-plain transition zone (Beijing, Tangshan, and Qinhuangdao) mainly experiences MHS (32%, 25%, and 37%, respectively) and SHS (53%, 62%, and 54%, respectively). While the southern plain zone suffers more and stronger heat stress, the VSHS percentage is higher, and Cangzhou, Langfang, and Hengshui experience the most. The average proportions of MHS, SHS, and VSHS were 13%, 54%, and 30% in Cangzhou, 12%, 57%, and 29% in Langfang, and 10%, 52%, 36% in Hengshui, respectively. At daytime, although more NTS occurs, a high percentage of cold stress is observed in the mountainous zone; Zhangjiakou and Chengde have 4% and 2% in MCS, 36% and 24% in SICS, respectively, and more in June (10% and 6% in MCS, 50% and 37% in SICS, respectively). In the southern plain zone, some cities still suffer a relatively high frequency of MHS. For instance, Hengshui has the highest frequency of 10% in summer, which increases to 16% in July. In some areas, the MHS frequency even reached 15% (Figure S3 in Supporting Information S1).

Figure 11 provides the annual trends of thermal stress category occurrences in each city in BTH. Maps of the trends are shown in Figures S4 and S5 in Supporting Information S1. Cities in the three parts show different typical characteristics. The northern mountainous zone (I) shows a decline in NTS and an increase in MHS and SHS during the daytime and a decline in MCS and SLCS and an increase in NTS at nighttime. The mountain plain zone (II) shows a decrease in MHS and an increase in SHS and VSHS during the daytime and a slight increase in MHS. The southern plain zone (III) presents the decline in MHS and SHS, whereas the increase in VSHS during the daytime, the decrease in NTS and the increase in MHS during the daytime. Eastern cities, like Tianjin, Cangzhou, Langfang, and Hengshui have the more increase of VSHS at daytime (3.86, 3.86, 4.97, and 3.66 d/10a, respectively), and more increase of MHS at nighttime (1.09, 1.34, 0.82, and 1.47 d/10a, respectively). Additionally, the junction of Tianjin, Langfang, and Cangzhou is found to have the most growth of VSHS frequency during the daytime (>5.00 d/10a, Figure S4 in Supporting Information S1), indicating much unfavorable conditions in summer with more and stronger heat stress. The increase in NTS at nighttime may partly improve the bioclimatic conditions, especially in Zhangjiakou and Chengde, where the growth rates were up to 2.11 and

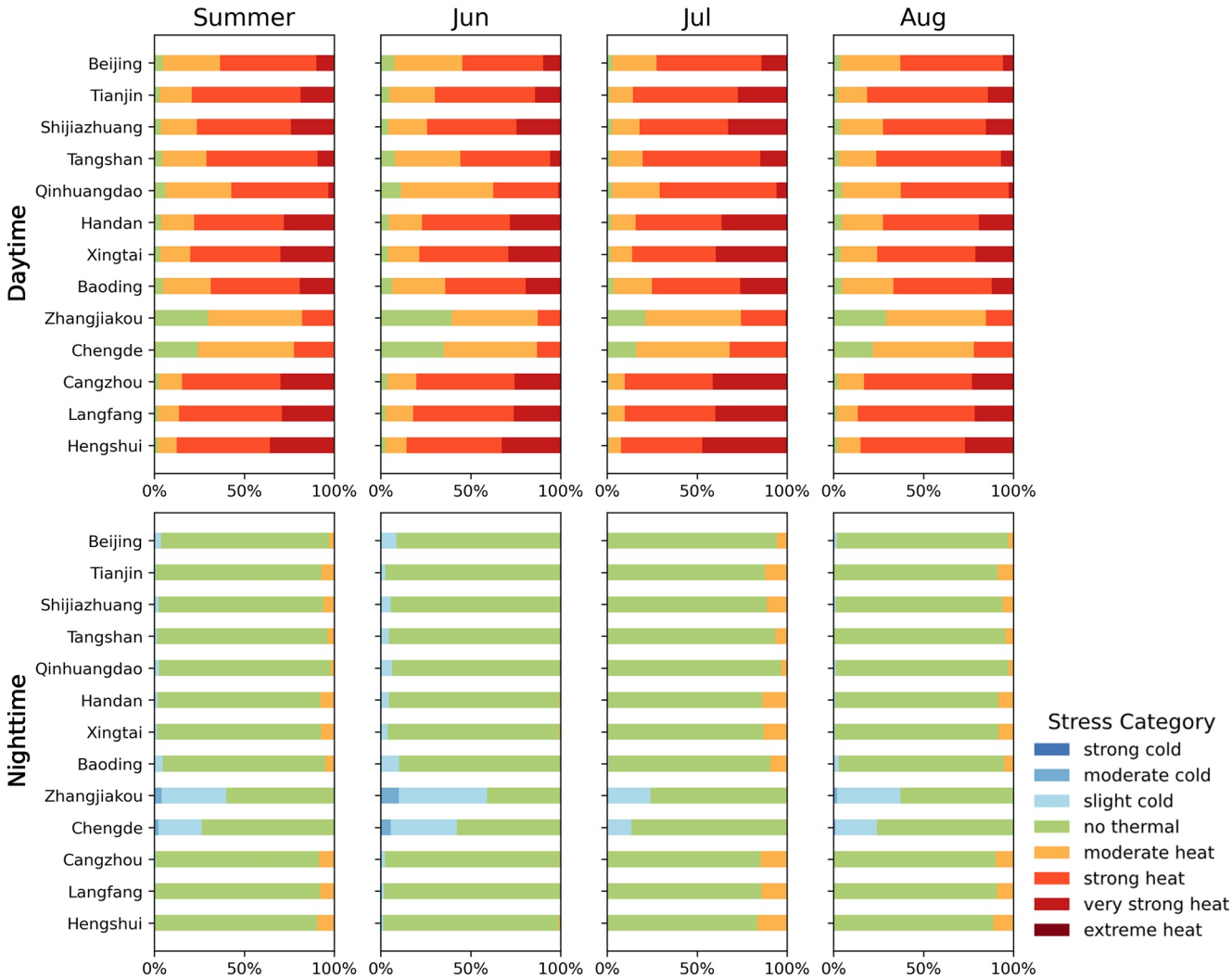

Figure 10. Averaged frequencies of thermal stress categories at daytime and nighttime in cities in Beijing-Tianjin-Hebei.

0.80 d/10a, respectively. Same as the result in BTH, the annual trends (in times) of frequency ratios of thermal stress to MHS at daytime and NTS at nighttime in cities were showed in Figure S6 in Supporting Information S1. At summer daytime, compare to the MHS, it could be confirmed that NTS decreased and MHS increased generally in the northern mountainous zone (I); both SHS and VSHS increased generally in the mountain plain zone (II); and VSHS greatly increased while SHS decreased generally in the southern plain zone (III). At summer nighttime, compare to the NTS, both MCS and SICS greatly decreased in the northern mountainous zone (I); SICS decreased and MHS increased generally in the mountain plain zone (II); and MHS greatly increased generally in the southern plain zone (III).

3.3. OTC at the City Scale Assessed by CTCS

Figure 12 shows the overall all-day, daytime, and nighttime OTC types according to averaged CTCS in the BTH. The embedded line charts in Figure 12 demonstrate the annual changes of CTCSs of each city in summer. Cities are clustered into four relative OTC types according to the cluster analysis of CTCS. In order of CTCS from high to low, the four groups are (I) comfortable, (II) less comfortable, (III) less uncomfortable, and (IV) uncomfortable. The numbers on the map represent rankings to CTCSs of cities.

For the daytime OTC (Figure 12a), the comfortable-type cities are in the northern mountainous zone (Chengde and Zhangjiakou). The less comfortable-type cities include Baoding and cities in the mountainous-plain transition

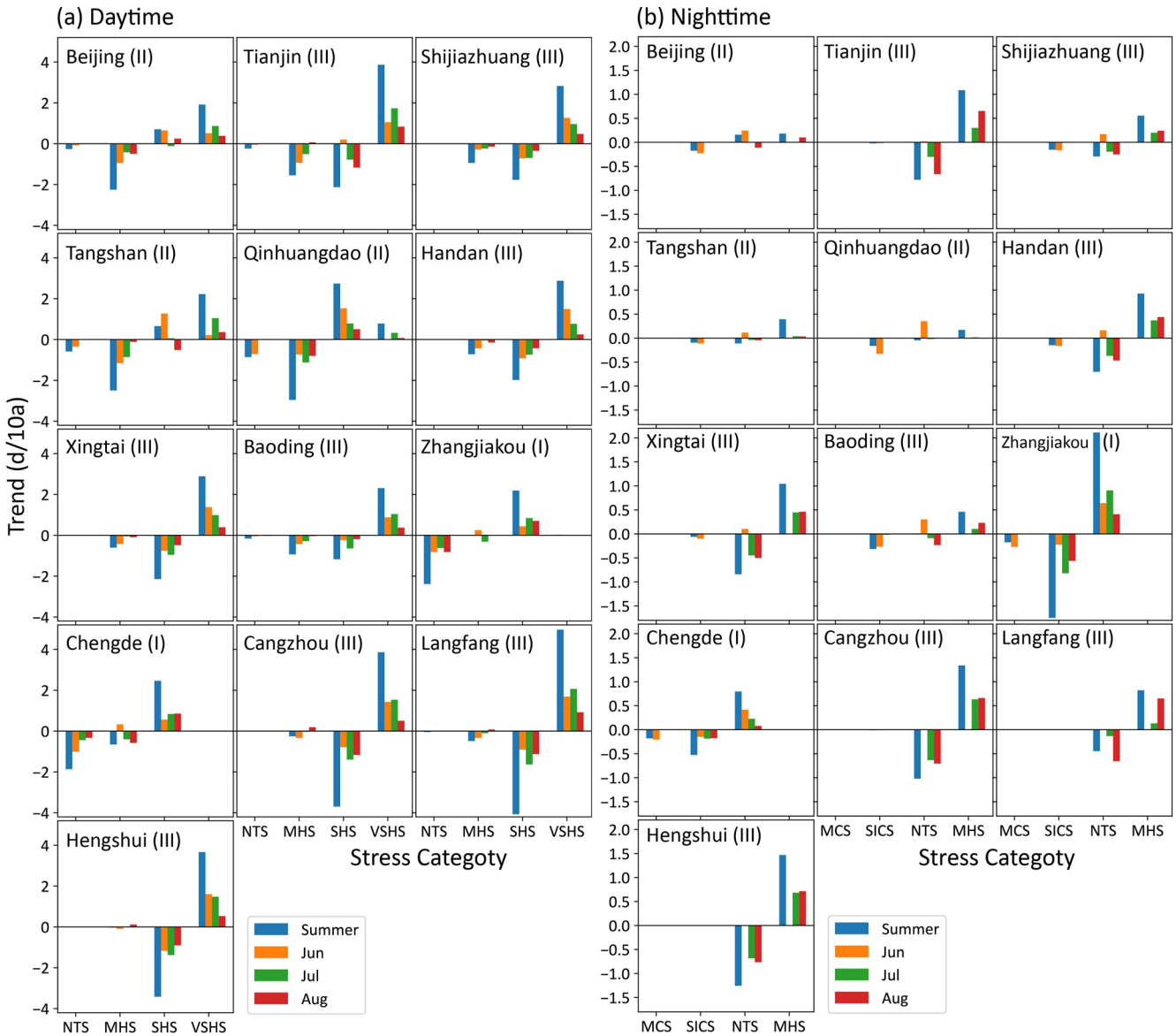

Figure 11. Annual trends (in days) of thermal stress categories at (a) daytime and (b) nighttime in cities in Beijing-Tianjin-Hebei.

zone (Beijing, Tangshan, and Qinhuangdao). The less-uncomfortable-type cities are Tianjin, Shijiazhuang, Xingtai, and Handan. The uncomfortable-type cities are Langfang, Cangzhou, and Hengshui, owing to their lowest CTCSs. From the perspective of nighttime OTCs, all the cities have positive CTCSs, which means that BTH is usually comfortable at night (Figure 12b). Nevertheless, the relative OTC types of the cities in BTH were dramatically inverse. Zhangjiakou and Chengde change to the uncomfortable type, meaning they are relatively uncomfortable at night since more cold stress occurs due to high altitude. Although Langfang, Cangzhou, Hengshui, Xingtai, and Handan are located in the plain zone and changed to Less-uncomfortable-type, they still have relatively low OTCs since suffering more MHS at night. Tianjin, Baoding, and Shijiazhuang are less comfortable. The best OTC is located in the mountainous-plain transition zone (Beijing, Tangshan, and Qinhuangdao) due to light cold and heat stress at night. The pattern of all-day OTCs was similar to that of daytime OTCs, with only a change in Baoding from the Less-comfortable-type to the Less-uncomfortable-type (Figure 12c), indicating worse OTCs in the all-day period than in the daytime.

Both the all-day OTC and daytime OTC present a north-south decreasing gradient pattern, and the similarity between them indicates that the daytime OTC dominates the OTC at the city scale in BTH. Generally, Zhangjiakou

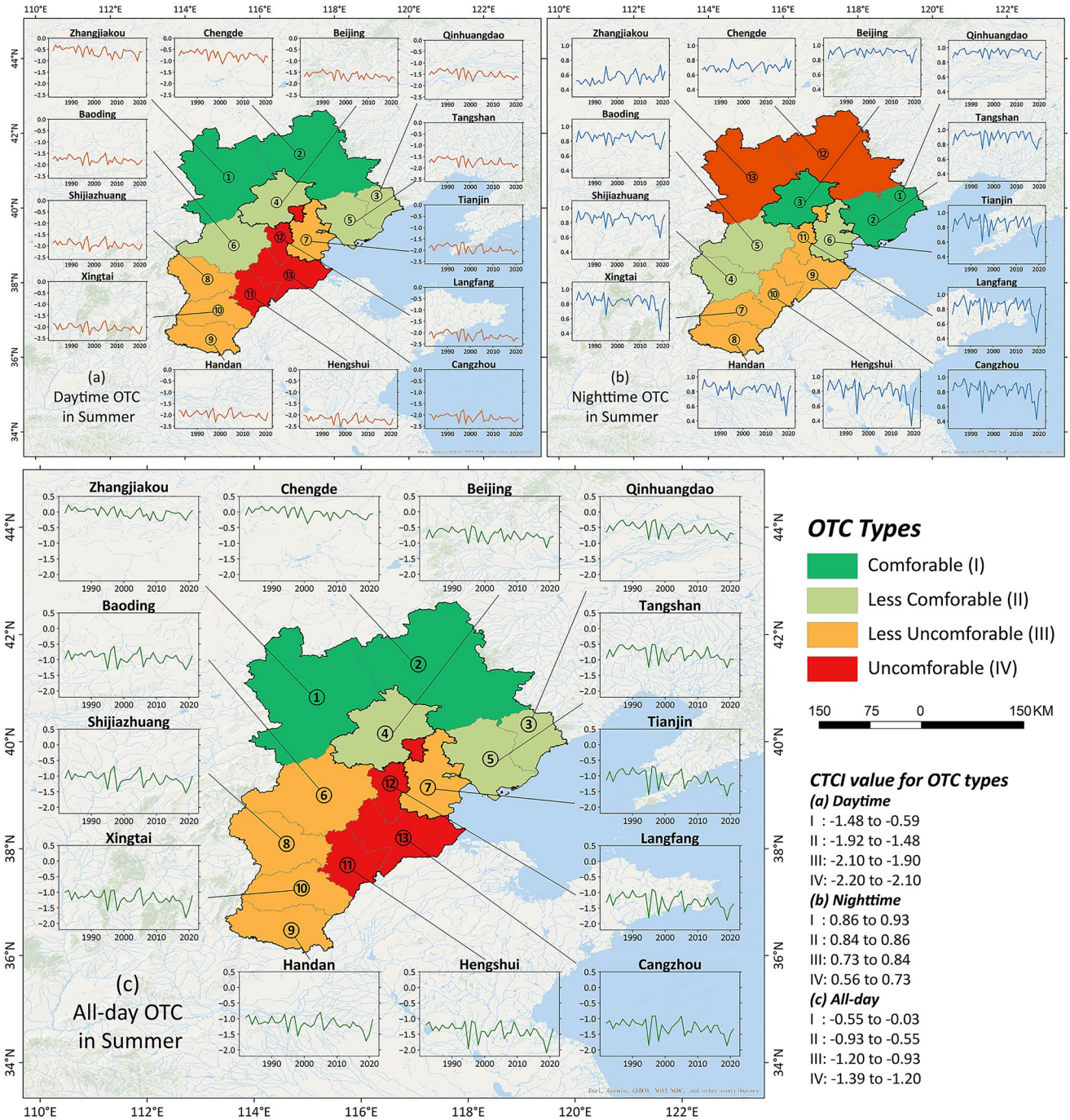

Figure 12. Maps of Outdoor thermal comfort types and time series of annual mean Composite Thermal Comfort Score in (a) all-day, (b) daytime, and (c) nighttime for cities in Beijing-Tianjin-Hebei during 1981–2020.

and Chengde were the two most comfortable cities in summer, with the highest all-day CTCS (−0.03, −0.03, respectively), even though their nighttime CTCSs (0.56, 0.71, respectively) were lower than those of other cities due to more MCS and SICS frequencies. In contrast, Langfang, Cangzhou, and Hengshui are the most uncomfortable cities with the lowest all-day CTCS (−2.10, −2.12, −2.20, respectively) since more heat stress occurs both at daytime and nighttime.

For months, the OTCs of cities also show a north-south gradient and vary by month and the time of day (Figure S7 in Supporting Information S1). July was the most unfavorable period with the lowest CTCS. The OTCs in June

were generally better than those in August, while those in the northern mountainous zone need to be compared at different times of day. In the northern mountainous zone, June had a better OTC during the daytime and a lower OTC at nighttime since it is cooler during the daytime and colder at nighttime.

Furthermore, the temporal changes in the annual summer CTCSs of each city in BTH are provided in the subgraphs in Figure 12 and Figure S6 in Supporting Information S1, and the decreasing trends in most cities were manifested. At nighttime, Zhangjiakou and Chengde show a different pattern against other cities, with much lower CTCS and increasing trends. Differences were more prominent on June and July nights (Figure S8 in Supporting Information S1). On June nights, the growth trends are mirrored in all cities and more obvious in Zhangjiakou and Chengde. On July nights, only Zhangjiakou and Chengde presented growth trends. These findings suggested that the OTC in BTH was getting worse except for the nights in the northern mountainous zones. The increasing UTCI and the decline in cold stress days at night was the reason for the improved OTC in northern mountainous zones, especially in June. The increase in UTCI and heat stress frequency resulted in much worse OTCs in the southern plain zones, such as Cangzhou and Hengshui, and was even more serious at night (Figure 12).

Additionally, several typical years (e.g., 1994, 1997, 2000, and 2018) have much worse OTCs than others. In contrast, these years had a much higher UTCI (33.2°C, 33.2°C, 33.2°C, 33.2°C, and 33.4°C during the daytime; 18.5°C, 16.7°C, 17.4°C, and 18.7°C at nighttime, respectively) and a higher frequency of heat stress (94%, 90%, 93%, and 94% during the daytime; 8%, 5%, 3%, and 11% at nighttime). This was especially the case in 1994 and 2018, which had the highest UTCI and the highest frequency of heat stress over the past 40 years both during the daytime and nighttime. Such bioclimatic conditions resulted in the worst OTCs over the past 40 years, especially at night in the southern plain zone. However, the OTC is even better in the northern mountainous zone since the decline in cold stress days at night.

4. Discussion

4.1. The Spatiotemporal Pattern of UTCI, Thermal Stress Categories, and CTCS in the BTH

Taking the BTH urban agglomeration as the study area, we proposed a summarized score based on the daily thermal stress levels assessed by the UTCI, called CTCS, to assess the daytime, nighttime, and all-day OTCs of cities in BTH over the past 40 years (1981–2020). The general daytime, nighttime, and all-day OTCs of cities in BTH evaluated by the averaged CTCSs show a north-south gradient pattern dominated by the tremendous topographic differences in BTH. Three topographic areas (the northern mountainous zone, the mountain-plain transition zone, and the southern plain zone) present different characteristics of spatial and temporal patterns in regional OTCs. The northern mountainous zone, including the cities of Zhangjiakou and Chengde, has the best overall OTC at daytime and all-day with the lowest general UTCI and heat stress frequency, while it inversely has the worst OTC at nighttime since they even suffer several cold stresses in the summer night. The mountain-plain transition zone, including Beijing, Tangshan, and Qinhuangdao, has relatively less comfortable conditions at daytime and all-day, while it has the best overall OTC at nighttime due to light cold and heat stress at night. The southern plain zone has a worse OTC both at daytime and nighttime, and consequently at all-day. Hengshui, Langfang, and Cangzhou are the cities with the worst overall OTCs. July is the most unfavorable month in summer regardless of daytime or nighttime, and June is generally the most comfortable, while June nights in the northern mountainous zone may be less comfortable with more and stronger cold stress.

From a specific and bioclimatic perspective, the UTCI shows a similar spatial pattern to CTCS. During the daytime, the OTC in BTH is unfavorable, with a high average UTCI (32°C) and a high frequency of severe heat stress (42% and 10% in SHS and VSHS). Conditions in southern cities are even worse, with higher heat stress than the northern cities. Zhangjiakou has the lowest average UTCI (27.9°C) and low severe heat stress frequency (17% and 0% in SHS and VSHS). Furthermore, Hengshui has the highest average UTCI (36.3°C) and high severe heat stress frequency (52% and 36% in SHS and VSHS). July has the worst OTC, and the frequency of SHS, and VSHS are up to 47% and 14% in BTH. In contrast, the summer night in BTH is much cooler and more favorable. The averaged UTCI is 16°C, and NTS conditions are prevalent (85% in frequency). Cold stress (12%) even occurs more frequently than heat stress (3%), especially in June (20% of cold stress while no heat stress occurs). However, cold stress mainly occurs in the northern mountainous zone, and areas in the southern plain zone still suffer a relatively high frequency of MHS (up to 15%). The results of UTCI and thermal stress frequency also support the evaluation of OTC assessed by CTCS.

4.2. The Trend of UTCI, Thermal Stress Categories, and CTCS in the BTH

The annual CTCS reveals that the OTC is deteriorating compounded day and night, which is in accordance with the change of UTCI and thermal stress frequency. During the daytime, the whole BTH region presented a decreasing trend in the CTCS, with the UTCI increasing by 0.32°C/10a and the VSHS and SHS frequencies increasing by 0.64 and 1.56 d/10a, respectively, representing more frequent and intense heat stress and more unfavorable bioclimatic conditions. The OTC in June worsened at a fast pace despite having the best overall OTC in summer, of which the increasing rate was 0.45°C/10a on UTCI days, 0.44 on SHS days, and 0.51 d/10a on VSHS days. The increase in July was also terrifying, with an increasing rate of 0.21°C/10a in UTCI and 0.66 d/10a in VSHS days, bringing a terrible truth that more and stronger deadly extreme heat has occurred over the past 40 years and poses a growing fatal threat to life, health and society. Additionally, the worsened OTC at nighttime poses a compounding threat to BTH, with an increasing rate of 0.21°C/10a in UTCI and 0.39 d/10a in MHS.

Moreover, the trend of UTCI and thermal stress levels put more emphasis on regional differences. The southern plain zones witness faster UTCI growth and stronger heat stress frequency compounded day and night, which will lead to more severe deadly threats (Di Napoli et al., 2018; Kuchcik, 2020). At the grid scale, the coastal areas west of Tianjin, south of Qinhuangdao and Tangshan, and north of Cangzhou are revealed with the highest growth of UTCI, especially in June and July. The southern part of Beijing, the junction of Tianjin, Langfang, and Cangzhou are found to have the most growth of VSHS frequency during the summer daytime, which is also the area with the most intense surface urban heat island in BTH from 2000 to 2015 (Chen et al., 2020). The warming effect of urbanization may be an important factor that worsens the OTC in the southern plain zones. Previous studies have assessed that the warming effect of urbanization prominently increasing heat events and human-perceived heat stress (Fu et al., 2022; Luo & Lau, 2018, 2021; Y. Wang et al., 2022). The southern plain is the primary zone for population distribution, economic activities, and agricultural production in BTH. While the deteriorating OTC aggravated by increasing heat stress frequency during the day and night here will greatly threaten human health, reduce outdoor work efficiency, and even knock out the water and electricity supply.

As for the northern mountainous zones, although the UTCIs are both increase in daytime and nighttime, the CTCS demonstrate the OTC varies differently at these two times of day. The increase of UTCI may improve the OTC due to the decrease in cold stress that mostly transform to NTS at nighttime. The decreasing cold stress frequency (−0.10 in MCS, −0.39 d/10a in SICS, respectively) and increasing NTS frequency (0.49 d/10a) in Zhangjiakou and Chengde at June night are more prominent than other cities, representing the more favorable bioclimatic conditions and result in an increasing OTC at June night. Conversely, the worsening of daytime and all-day OTCs cannot be ignored here. Zhangjiakou and Chengde show the fastest CTCSs decline at daytime, with trends of 0.38°C/10a and 0.33°C/10a in UTCIs, respectively. The growth of UTCI in the north of Zhangjiakou reaching more than 0.40°C/10a, which is the highest over the BTH. Consequently, the heat stress frequency also increased significantly at daytime. The northern areas with high altitudes mainly have more frequent MHS, while the south of the mountainous zones have more SHS occurs. Overall, Zhangjiakou and Chengde have trends of 2.19 in the MHS and 2.46 d/10a in the SHS. This phenomenon indicates that global warming may partly alleviate the cold stress and improve the OTC in mountainous areas at night, but generally worsen the OTC at daytime. As an important ecological protection and tourism destination in BTH, the high variability in OTC obviously raises new challenges and opportunities for the tourism development and ecology protection.

4.3. Limitations

This study also had some limitations. The proposed CTCS only provides relative values for the comparison of OTCs between different regions over the same spatiotemporal scale, while the CTCS value did not have specific physical meanings, such as UTCI, that can be numerically divided into thermal stress categories. Additionally, the four OTC types from comfortable to uncomfortable were obtained based on the relative value of the data series, which only makes comparisons sense over the same time periods.

5. Conclusions

This study quantitatively assessed the long-term, summertime, regional OTC in BTH urban agglomeration from 1981 to 2020. The general OTCs of cities show a decreasing north-south gradient pattern dominated by the tremendous topographic differences in BTH. For all-day and daytime OTCs, the northern mountainous zone

(Zhangjiakou and Chengde) presents the best OTCs. Then, the mountain-plain transition zone (Qinhuangdao, Beijing, and Tangshan) shows a moderate OTC. The southern plain zone shows the worst OTC and could be clustered into two categories. Hengshui, Langfang, and Cangzhou show the worst OTCs since they experience increasingly stronger heat stress in summer. At nighttime, the best OTC areas were in the mountain-plain transition zone, while the northern mountainous zone exhibits the worst OTC since more cold stress occurred.

The higher UTCI, increasing frequency of heat stress, and the ensuing worsening OTC that even compounded day and night indicate that the climate-driven negative effects were much stronger over the past 40 years in BTH. As for daytime, the increasing rate of UTCI is 0.32°C/10a, and that of heat stress frequency is 0.88 d/10a. As for nighttime, the growing rate of UTCI and heat stress frequency is 0.21°C/10a and 0.39 d/10a, respectively. Accelerating worsening OTC occurred in the southern plain zone with faster UTCI growth and stronger heat stress frequency compounded day and night. The northern mountainous zone conditions are reversed during the daytime and nighttime. Zhangjiakou and Chengde show the fastest CTCSs decline at the daytime, with trends of 0.38°C/10a and 0.33°C/10a in UTCIs, respectively. While the increase in UTCI may partly improve the OTC at night since cold stress decreased, that mainly transform to NTS. The increasing temperature and urban heat island driven by climate change and urbanization may be the culprit for the deterioration of OTC. Climate change adaptation strategies are needed to ensure urban and ecological resilience.

Compared to the traditional heatwave research that mainly focuses on the temperature, the assessments of bioclimatic conditions are more considerable to take more relevant meteorological parameters into account, which is an essential basis for effective evaluation of the impacts of global change and extreme heat on human health and behavior, as well as on the social economy. Though UTCI has 10 years of applications, the assessment of bioclimatic conditions still facing many problems, and long-term analyses that consider the intensity, duration, and extent of thermal stress both day and night for urban areas are lacking. We hope the study will better understand the bioclimatic conditions in BTH and support decision-makers to improve OTC and reduce related health risks.

Conflict of Interest

The authors declare no conflicts of interest relevant to this study.

Data Availability Statement

Data sets for this research are publicly available. Meteorological data are available from the ERA5 (https://cds.climate.copernicus.eu/cdsapp#!/dataset/reanalysis-era5-pressure-levels?tab=overview) and ERA5-Land data sets (https://cds.climate.copernicus.eu/cdsapp#!/dataset/reanalysis-era5-land?tab=overview).

Acknowledgments
Supported by the National Key Research and Development Plan of China (2019YFA0606901), the Strategic Priority Research Program of the Chinese Academy of Sciences (XDA23100303), and the China Postdoctoral Science Foundation (2022T150057).

References

Adrian, S.-C., Sergiu, C., Maria, M., Anca, S.-C., & Monica, M. (2008). Models for the indices of thermal comfort. *Journal of Medicine and Life*, *1*(2), 148.

Arias, P., Bellouin, N., Coppola, E., Jones, R., Krinner, G., Marotzke, J., et al. (2021). Climate change 2021: The physical science basis. In *Contribution of working Group 14 I to the sixth assessment report of the intergovernmental panel on climate change*. Technical Summary.

Asghari, M., Teimori, G., Abbasinia, M., Shakeri, F., Tajik, R., Ghannadzadeh, M. J., & Ghalhari, G. F. (2019). Thermal discomfort analysis using UTCI and MEMI (PET and PMV) in outdoor environments: Case study of two climates in Iran (Arak & Bandar Abbas). *Royal Meteorological Society*, *74*(S1), S57–S64. https://doi.org/10.1002/wea.3612

Baaghideh, M., Mayvaneh, F., Shekari Badi, A., & Shojaee, T. (2016). Evaluation of human thermal comfort using UTCI index: Case study Khorasan Razavi, Iran. *Natural Environment Change*, *2*(2), 165–175.

Bian, Y. J., Sun, P., Zhang, Q., Luo, M., & Liu, R. L. (2022). Amplification of non-stationary drought to heatwave duration and intensity in eastern China: Spatiotemporal pattern and causes. *Journal of Hydrology*, *612*, 128154. https://doi.org/10.1016/j.jhydrol.2022.128154

Blazejczyk, K. (2001). Assessment of recreational potential of bioclimate based on the human heat balance. In *Proceedings of the First International Workshop on Climate, Tourism and Recreation. Report of a Workshop*, (pp. 133–152).

Blazejczyk, K. (2021). UTCI-10 years of applications. *International Journal of Biometeorology*, *65*(9), 1461–1462. https://doi.org/10.1007/s00484-021-02174-1

Błażejczyk, K., Broede, P., Fiala, D., Havenith, G., Holmér, I., Jendritzky, G., et al. (2010). Principles of the new Universal Thermal Climate Index (UTCI) and its application to bioclimatic research in European scale. *Miscellanea Geographica*, *14*(2010), 91–102. https://doi.org/10.2478/mgrsd-2010-0009

Blazejczyk, K., Epstein, Y., Jendritzky, G., Staiger, H., & Tinz, B. (2011). Comparison of UTCI to selected thermal indices. *International Journal of Biometeorology*, *56*(3), 515–535. https://doi.org/10.1007/s00484-011-0453-2

Błażejczyk, K., Jendritzky, G., Bröde, P., Fiala, D., Havenith, G., Epstein, Y., et al. (2013). An introduction to the universal thermal climate index (UTCI). *Geographia Polonica*, *86*(1), 5–10. https://doi.org/10.7163/gpol.2013.1

Błażejczyk, K., Kuchcik, M., Błażejczyk, A., Milewski, P., & Szmyd, J. (2014). Assessment of urban thermal stress by UTCI–experimental and modelling studies: An example from Poland. *Journal of the Geographical Society of Berlin*, *145*(1–2), 16–33. https://doi.org/10.12854/erde-145-3

Brode, P., Fiala, D., Blazejczyk, K., Holmer, I., Jendritzky, G., Kampmann, B., et al. (2012). Deriving the operational procedure for the universal thermal climate index (UTCI). *International Journal of Biometeorology*, *56*(3), 481–494. https://doi.org/10.1007/s00484-011-0454-1

Bröde, P., Krüger, E. L., Rossi, F. A., & Fiala, D. (2012). Predicting urban outdoor thermal comfort by the Universal Thermal Climate Index UTCI—A case study in Southern Brazil. *International Journal of Biometeorology*, *56*(3), 471–480. https://doi.org/10.1007/s00484-011-0452-3

Burke, M., Hsiang, S. M., & Miguel, E. (2015). Global non-linear effect of temperature on economic production. *Nature*, *527*(7577), 235–239. https://doi.org/10.1038/nature15725

Chen, J. (2019). The population of the Beijing-Tianjin-Hebei region has increased by more than 13 million in the past decade: The increase of Beijing and Tianjin exceeded 7.5 million, but the aging population is serious, 21st century business Herald. Retrieved from https://baijiahao.baidu.com/s?id=1653939407965595897%26wfr=spider%26for=pc

Chen, M., Zhou, Y., Hu, M., & Zhou, Y. (2020). Influence of urban scale and urban expansion on the urban heat island effect in metropolitan areas: Case study of Beijing-Tianjin-Hebei urban agglomeration. *Remote Sensing*, *12*(21), 3491. https://doi.org/10.3390/rs12213491

Coccolo, S., Kämpf, J., Scartezzini, J.-L., & Pearlmutter, D. (2016). Outdoor human comfort and thermal stress: A comprehensive review on models and standards. *Urban Climate*, *18*, 33–57. https://doi.org/10.1016/j.uclim.2016.08.004

Di Napoli, C., Barnard, C., Prudhomme, C., Cloke, H. L., & Pappenberger, F. (2020). ERA5-HEAT: A global gridded historical dataset of human thermal comfort indices from climate reanalysis. *Geoscience Data Journal*, *8*(1), 1–9. https://doi.org/10.1002/gdj3.102

Di Napoli, C., Hogan, R. J., & Pappenberger, F. (2020). Mean radiant temperature from global-scale numerical weather prediction models. *International Journal of Biometeorology*, *64*(7), 1233–1245. https://doi.org/10.1007/s00484-020-01900-5

Di Napoli, C., Pappenberger, F., & Cloke, H. L. (2018). Assessing heat-related health risk in Europe via the Universal Thermal Climate Index (UTCI). *International Journal of Biometeorology*, *62*(7), 1155–1165. https://doi.org/10.1007/s00484-018-1518-2

Dosio, A. (2017). Projection of temperature and heat waves for Africa with an ensemble of CORDEX regional climate models. *Climate Dynamics*, *49*(1), 493–519. https://doi.org/10.1007/s00382-016-3355-5

Dosio, A., Mentaschi, L., Fischer, E. M., & Wyser, K. (2018). Extreme heat waves under 1.5 C and 2 C global warming. *Environmental Research Letters*, *13*(5), 054006. https://doi.org/10.1088/1748-9326/aab827

ECMWF. (2019). ERA5-Land: Data documentation. Retrieved from https://confluence.ecmwf.int/display/CKB/ERA5%2DLand3A%2Bdata%2Bdocumentation%23ERA5Land%3AdatadocumentationaccumulationsAccumulations

Fanger, P. O. (1970). Thermal comfort. Analysis and applications in environmental engineering. In *Thermal comfort. Analysis and applications in environmental engineering*, (p. 244).

Fiala, D., Havenith, G., Bröde, P., Kampmann, B., & Jendritzky, G. (2012). UTCI-Fiala multi-node model of human heat transfer and temperature regulation. *International Journal of Biometeorology*, *56*(3), 429–441. https://doi.org/10.1007/s00484-011-0424-7

Fu, X., Yao, L., & Sun, S. (2022). Accessing the heat exposure risk in Beijing-Tianjin-Hebei region based on heat island footprint analysis. *Atmosphere*, *13*(5), 739. https://doi.org/10.3390/atmos13050739

Gagge, A., Fobelets, A., & Berglund, P. (1986). A standard predictive index of human response to the thermal environment. *ASHRAE Transactions*, *92*, 709–731.

Geletič, J., Lehnert, M., & Jurek, M. (2020). Spatiotemporal variability of air temperature during a heat wave in real and modified landcover conditions: Prague and Brno (Czech Republic). *Urban Climate*, *31*, 100588. https://doi.org/10.1016/j.uclim.2020.100588

Gonzalez, R., Nishi, Y., & Gagge, A. (1974). Experimental evaluation of standard effective temperature a new biometeorological index of man's thermal discomfort. *International Journal of Biometeorology*, *18*(1), 1–15. https://doi.org/10.1007/bf01450660

Havenith, G., Fiala, D., Błazejczyk, K., Richards, M., Bröde, P., Holmér, I., et al. (2012). The UTCI-clothing model. *International Journal of Biometeorology*, *56*(3), 461–470. https://doi.org/10.1007/s00484-011-0451-4

Hersbach, H., Bell, B., Berrisford, P., Biavati, G., Horányi, A., Muñoz Sabater, J., et al. (2018). ERA5 hourly data on pressure levels from 1959 to present. *Copernicus Climate Change Service (C3S) Climate Data Store (CDS)*, *10*. https://doi.org/10.24381/cds.bd0915c6

Hou, L., Yue, W., & Liu, X. (2021). Spatiotemporal patterns and drivers of summer heat island in Beijing-Tianjin-Hebei Urban Agglomeration, China. *IEEE Journal of Selected Topics in Applied Earth Observations and Remote Sensing*, *14*, 7516–7527. https://doi.org/10.1109/jstars.2021.3094559

International Standards Organization (ISO). (2004). Ergonomics of the thermal environment: Analytical determination and interpretation of heat stress using calculation of the predicted heat strain. ISO Standards 7933.

Jendritzky, G., de Dear, R., & Havenith, G. (2012). UTCI—Why another thermal index? *International Journal of Biometeorology*, *56*(3), 421–428. https://doi.org/10.1007/s00484-011-0513-7

Jendritzky, G., Havenith, G., Weihs, P., Batchvarova, E., & DeDear, R. (2008). The universal thermal climate index UTCI—Goal and state of COST action 730 and ISB commission 6. In *Proceedings 18th International Congress of Biometeorology (ICB)*, (pp. 22–26).

Jendritzky, G., Maarouf, A., Fiala, D., & Staiger, H. (2002). An update on the development of a universal thermal climate index. In *15th Conference on Biometeorology Aerobiology and 16th ICB02*, (Vol. *27*, pp. 129–133).

Jendritzky, G., Menz, G., Schirmer, H., & Schmidt-Kessen, W. (1990). Methodik zur R äumlichen Bewertung der Thermischen Komponente im Bioklima des Menschen. In *Beiträge der Akademie für Raumforschung und Landesplanung*, (Vol. *114*).

Kang, S., & Eltahir, E. A. (2018). North China Plain threatened by deadly heatwaves due to climate change and irrigation. *Nature Communications*, *9*(1), 1–9. https://doi.org/10.1038/s41467-018-05252-y

Kendall, M. G. (1975). *Rank correlation methods*. Griffin.

Koppe, C., Kovats, S., Jendritzky, G., & Menne, B. (2004). *Heat-waves: Risks and responses*. World Health Organization. Regional Office for Europe.

Koteswara Rao, K., Lakshmi Kumar, T., Kulkarni, A., Ho, C.-H., Mahendranath, B., Desamsetti, S., et al. (2020). Projections of heat stress and associated work performance over India in response to global warming. *Scientific Reports*, *10*(1), 1–14. https://doi.org/10.1038/s41598-020-73245-3

Krzyżewska, A., Wereski, S., & Dobek, M. (2020). Summer UTCI variability in Poland in the twenty-first century. *International Journal of Biometeorology*, *65*(9), 1–17. https://doi.org/10.1007/s00484-020-01965-2

Kuchcik, M. (2017). Thermal conditions in Poland at the turn of the 20th and 21st centuries, and their impact on mortality. *Geographical Studies*, *263*. 1-10

Kuchcik, M. (2020). Mortality and thermal environment (UTCI) in Poland—Long-term, multi-city study. *International Journal of Biometeorology*, *65*(9), 1–13. https://doi.org/10.1007/s00484-020-01995-w

Lei, Y., Zhang, X., & Zhao, X. (2020). Spatial-temporal distribution characteristics of comfort index of human body in Shaanxi Province from 1971 to 2018. *Arid Land Geography*, *43*(6), 1417–1425. Chinese. https://doi.org/10.12118/j.issn.1000-6060.2020.06.02

Leroyer, S., Bélair, S., Spacek, L., & Gultepe, I. (2018). Modelling of radiation-based thermal stress indicators for urban numerical weather prediction. *Urban Climate*, *25*, 64–81. https://doi.org/10.1016/j.uclim.2018.05.003

Li, J., Niu, J., Mak, C. M., Huang, T., & Xie, Y. (2018). Assessment of outdoor thermal comfort in Hong Kong based on the individual desirability and acceptability of sun and wind conditions. *Building and Environment*, *145*, 50–61. https://doi.org/10.1016/j.buildenv.2018.08.059

Li, P. F., Liu, W. J., & Zhao, X. Y. (2015). The changes of atmospheric temperature, precipitation and potential evapotranspiration in Beijing-Tianjin-Hebei region in recent 50 years. *Journal of Arid Land Resources & Environment*, *29*(3), 137–143. (in Chinese).

Li, Q., Sheng, B., Huang, J., Li, C., Song, Z., Chao, L., et al. (2022). Different climate response persistence causes warming trend unevenness at continental scales. *Nature Climate Change*, *12*(4), 1–7. https://doi.org/10.1038/s41558-022-01313-9

Liu, Y., Li, H., Gao, P., & Zhong, C. (2020). Monitoring the detailed dynamics of regional thermal environment in a developing urban agglomeration. *Sensors*, *20*(4), 1197. https://doi.org/10.3390/s20041197

Luo, M., & Lau, N. C. (2018). Increasing heat stress in urban areas of eastern China: Acceleration by urbanization. *Geophysical Research Letters*, *45*(23), 13060–13069. https://doi.org/10.1029/2018gl080306

Luo, M., & Lau, N. C. (2021). Increasing human-perceived heat stress risks exacerbated by urbanization in China: A comparative study based on multiple metrics. *Earth's Future*, *9*(7), e2020EF001848. https://doi.org/10.1029/2020ef001848

Ma, F., & Yuan, X. (2021). More persistent summer compound hot extremes caused by global urbanization. *Geophysical Research Letters*, *48*(15), e2021GL093721. https://doi.org/10.1029/2021gl093721

Ma, F., Yuan, X., Jiao, Y., & Ji, P. (2020). Unprecedented Europe heat in June–July 2019: Risk in the historical and future context. *Geophysical Research Letters*, *47*(11), e2020GL087809. https://doi.org/10.1029/2020gl087809

Mann, H. B. (1945). Nonparametric tests against trend. *Econometrica: Journal of the Econometric Society*, *13*(3), 245–259. https://doi.org/10.2307/1907187

Matzarakis, A., Rutz, F., & Mayer, H. (2007). Modelling radiation fluxes in simple and complex environments—Application of the RayMan model. *International Journal of Biometeorology*, *51*(4), 323–334. https://doi.org/10.1007/s00484-006-0061-8

Mayer, H., & Höppe, P. (1987). Thermal comfort of man in different urban environments. *Theoretical and Applied Climatology*, *38*(1), 43–49. https://doi.org/10.1007/bf00866252

Milovanović, J. (2020). UTCI based assessment of urban outdoor thermal comfort in Belgrade, Serbia. In *Sinteza 2020-International Scientific Conference on Information Technology and Data Related Research* (pp. 70–77). Singidunum University.

Mohammadi, B., Gholizadeh, M., & Alijani, B. (2018). Spatial distribution of thermal stresses in Iran based on PET and UTCI indices. *Applied Ecology and Environmental Research*, *16*(5), 5423–5445. https://doi.org/10.15666/aeer/1605_54235445

Mourato, S., Moreira, M., & Corte-Real, J. (2010). Interannual variability of precipitation distribution patterns in Southern Portugal. *International Journal of Climatology*, *30*(12), 1784–1794. https://doi.org/10.1002/joc.2021

Müller, M. (2007). Dynamic time warping. Information retrieval for music and motion (pp. 69–84).

Muñoz Sabater, J. (2019). ERA5-Land hourly data from 1981 to present. *Copernicus Climate Change Service (C3S) Climate Data Store (CDS)*, *10*. https://doi.org/10.24381/cds.e2161bac

Nalley, D., Adamowski, J., Khalil, B., & Ozga-Zielinski, B. (2013). Trend detection in surface air temperature in Ontario and Quebec, Canada during 1967–2006 using the discrete wavelet transform. *Atmospheric Research*, *132*, 375–398. https://doi.org/10.1016/j.atmosres.2013.06.011

National Oceanic and Atmospheric Administration (NOAA). (1997). NOAA global vegetation index user's guide APPENDIX L: Software to calculate relative azimuth from third generation weekly composite GVI date. Retrieved from http://www2.ncdc.noaa.gov/docs/gviug/html/l/app-l.htm

Okoniewska, M. (2020). Daily and seasonal variabilities of thermal stress (based on the UTCI) in air masses typical for central Europe: An example from Warsaw. *International Journal of Biometeorology*, *65*(9), 1–10. https://doi.org/10.1007/s00484-020-01997-8

Park, C. E., & Jeong, S. (2022). Population exposure projections to intensified summer heat. *Earth's Future*, *10*(2), e2021EF002602. https://doi.org/10.1029/2021ef002602

Pecelj, M. M., Lukić, M. Z., Filipović, D. J., Protić, B. M., & Bogdanović, U. M. (2020). Analysis of the universal thermal climate index during heat waves in Serbia. *Natural Hazards and Earth System Sciences*, *20*(7), 2021–2036. https://doi.org/10.5194/nhess-20-2021-2020

Perkins-Kirkpatrick, S., & Lewis, S. (2020). Increasing trends in regional heatwaves. *Nature Communications*, *11*(1), 1–8. https://doi.org/10.1038/s41467-020-16970-7

Qin, D. H., Ding, Y. J., & Zhai, P. M. (2021). *Climate and ecological environment evolution in China: 2021 (Volume One Scientific Basis)*. Science Press. (in Chinese).

Sahabi Abed, S., & Matzarakis, A. (2018). Quantification of the tourism climate of Algeria based on the climate-tourism-information-scheme. *Atmosphere*, *9*(7), 250. https://doi.org/10.3390/atmos9070250

Sen, P. K. (1968). Estimates of the regression coefficient based on Kendall's tau. *Journal of the American Statistical Association*, *63*(324), 1379–1389. https://doi.org/10.1080/01621459.1968.10480934

Shen, S., Cheng, C., Song, C., Yang, J., Yang, S., Su, K., et al. (2018). Spatial distribution patterns of global natural disasters based on biclustering. *Natural Hazards*, *92*(3), 1809–1820. https://doi.org/10.1007/s11069-018-3279-y

Shi, Z., Xu, X., & Jia, G. (2021). Urbanization magnified nighttime heat waves in China. *Geophysical Research Letters*, *48*(15), e2021GL093603. https://doi.org/10.1029/2021gl093603

Si, P., Liang, D. P., Chen, K. H., & Luo, C. J. (2021). Urbanization effect on average and extreme temperature warming in Tianjin during the last 60 Years. *Climatic and Environmental Research*, *26*(2), 142–154.

Spencer, J. W. (1971). Fourier series representation of the position of the sun. *Search*, *2*(5), 162–172.

Stolwijk, J. A. (1971). *A mathematical model of physiological temperature regulation in man* (No. NASA-CR-1855). NASA.

Sun, G. L., Wang, X. Y., Zhang, X. P., Wu H. W., & Shen, L. (2011). Temporal-spatial characteristics of human comfort in Beijing-Tianjin-Hebei region. *Journal of Meteorology and Environment 27*(3), 18–23, Chinese

Sun, Y., Hu, T., Zhang, X., Li, C., Lu, C., Ren, G., & Jiang, Z. (2019). Contribution of global warming and urbanization to changes in temperature extremes in Eastern China. *Geophysical Research Letters*, *46*(20), 11426–11434. https://doi.org/10.1029/2019gl084281

Talhi, A., Barlet, A., Bruneau, D., & Aichour, B. (2020). Towards a prediction of outdoor human thermal comfort adapted for designers of urban spaces: Examining UTCI and APCI in the context of Algiers (Algeria). *International Journal of Biometeorology*, *64*(4), 1–12. https://doi.org/10.1007/s00484-019-01854-3

Thorsson, S., Lindberg, F., Eliasson, I., & Holmer, B. (2007). Different methods for estimating the mean radiant temperature in an outdoor urban setting. *International Journal of Biometeorology*, *27*(14), 1983–1993. https://doi.org/10.1002/joc.1537

Tomczyk, A. M., & Owczarek, M. (2020). Occurrence of strong and very strong heat stress in Poland and its circulation conditions. *Theoretical and Applied Climatology*, *139*(3), 893–905. https://doi.org/10.1007/s00704-019-02998-3

Vinogradova, V. (2020). Using the universal thermal climate index (UTCI) for the assessment of bioclimatic conditions in Russia. *International Journal of Biometeorology*, *65*(9), 1–11. https://doi.org/10.1007/s00484-020-01901-4

Wang, J., Chen, Y., Liao, W., He, G., Tett, S. F., Yan, Z., et al. (2021). Anthropogenic emissions and urbanization increase risk of compound hot extremes in cities. *Nature Climate Change*, *11*(12), 1084–1089. https://doi.org/10.1038/s41558-021-01196-2

Wang, Y., Xiang, Y., Song, L., & Liang, X.-Z. (2022). Quantifying the contribution of urbanization to summer extreme high-temperature events in the Beijing-Tianjin-Hebei urban agglomeration. *Journal of Applied Meteorology and Climatology*, *61*(6), 669–683. https://doi.org/10.1175/jamc-d-21-0201.1

Weihs, P., Staiger, H., Tinz, B., Batchvarova, E., Rieder, H., Vuilleumier, L., et al. (2012). The uncertainty of UTCI due to uncertainties in the determination of radiation fluxes derived from measured and observed meteorological data. *International Journal of Biometeorology*, *56*(3), 537–555. https://doi.org/10.1007/s00484-011-0416-7

Woan, G. (2000). Astrophysics. In *The Cambridge handbook of physics formulas*. Cambridge University Press.

Wu, S., Wang, P., Tong, X., Tian, H., Zhao, Y., & Luo, M. (2021). Urbanization-driven increases in summertime compound heat extremes across China. *Science of the Total Environment*, *799*, 149166. https://doi.org/10.1016/j.scitotenv.2021.149166

Yan, Y., Xu, Y., & Yue, S. (2021). A high-spatial-resolution dataset of human thermal stress indices over South and East Asia. *Scientific Data*, *8*(1), 229. https://doi.org/10.1038/s41597-021-01010-w

Yang, J., Zhou, M., Ren, Z., Li, M., Wang, B., Liu, D. L., et al. (2021). Projecting heat-related excess mortality under climate change scenarios in China. *Nature Communications*, *12*(1), 1–11. https://doi.org/10.1038/s41467-021-21305-1

Yao, R., Hu, Y. Q., Sun, P., Bian, Y. J., & Zhang, S. L. (2022). Effects of urbanization on heat waves based on the wet-bulb temperature in the Yangtze River Delta urban agglomeration, China. *Urban Climate*, *41*, 101067. https://doi.org/10.1016/j.uclim.2021.101067

Yazdanpanah, H., Barghi, H., & Esmaili, A. (2016). Effect of climate change impact on tourism: A study on climate comfort of Zayandehroud River route from 2014 to 2039. *Tourism Management Perspectives*, *17*, 82–89. https://doi.org/10.1016/j.tmp.2015.12.002

Zare, S., Shirvan, H. E., Hemmatjo, R., Nadri, F., Jahani, Y., Jamshidzadeh, K., & Paydar, P. (2019). A comparison of the correlation between heat stress indices (UTCI, WBGT, WBDT, TSI) and physiological parameters of workers in Iran. *Weather and Climate Extremes*, *26*, 100213. https://doi.org/10.1016/j.wace.2019.100213

Zhang, W. J., Zhang, B. P., Zhu, W. B., Tang, X. L., Li, F. J., Liu, X. S., & Yu, Q. (2021). Comprehensive assessment of MODIS-derived near-surface air temperature using wide elevation-spanned measurements in China. *Science of the Total Environment*, *800*, 149535. https://doi.org/10.1016/j.scitotenv.2021.149535

Zhang, Y., Li, Q., Ge, Y., Du, X., & Wang, H. (2022). Growing prevalence of heat over cold extremes with overall milder extremes and multiple successive events. *Communications Earth & Environment*, *3*(1), 1–13. https://doi.org/10.1038/s43247-022-00404-x

Zhao, M., Cheng, C., Zhou, Y., Li, X., Shen, S., & Song, C. (2022). A global dataset of annual urban extents (1992–2020) from harmonized nighttime lights. *Earth System Science Data*, *14*(2), 517–534. https://doi.org/10.5194/essd-14-517-2022

Zhe, M., Zhang, X. Q., Shen, P. K., & Hou, W. J. (2020). Spatial-temporal pattern of temperature variation in Beijing-Tianjin-Hebei region over the period 1957-2017. *Research of Soil and Water Conservation*, *27*(5), 194–201, Chinese

Zhou, L., Dickinson, R. E., Tian, Y., Fang, J., Li, Q., Kaufmann, R. K., et al. (2004). Evidence for a significant urbanization effect on climate in China. *Proceedings of the National Academy of Sciences of the United States of America*, *101*(26), 9540–9544. https://doi.org/10.1073/pnas.0400357101